NASA CR-159661
PWA-5515-87C

NASA

JT9D-70/59 IMPROVED HIGH PRESSURE TURBINE ACTIVE CLEARANCE CONTROL SYSTEM

by
W. O. Gaffin

UNITED TECHNOLOGIES CORPORATION
PRATT & WHITNEY AIRCRAFT GROUP
COMMERCIAL PRODUCTS DIVISION

Prepared for
NATIONAL AERONAUTICS AND SPACE ADMINISTRATION

NASA-Lewis Research Center
Contract NAS3-20630

1. Report No	2. Government Accession No	3. Recipient's Catalog No.
CR-159661		

4. Title and Subtitle	5. Report Date
JT9D-70/59 IMPROVED HIGH PRESSURE TURBINE ACTIVE CLEARANCE CONTROL SYSTEM	September 17, 1979
	6. Performing Organization Code
7. Author(s)	8. Performing Organization Report No
W. O. Gaffin	PWA-5515-87C
	10. Work Unit No.
9. Performing Organization Name and Address UNITED TECHNOLOGIES CORPORATION Pratt & Whitney Aircraft Group Commercial Products Division East Hartford, Connecticut 01608	11. Contract or Grant No. NAS3-20630
	13. Type of Report and Period Covered Contractor Report
12. Sponsoring Agency Name and Address NASA - Lewis Research Center 21000 Brookpark Rd. Cleveland, Ohio 44135	14 Sponsoring Agency Code

15. Supplementary Notes

Project Manager, Joseph A. Ziemianski — Project Engineer, Thomas N. Strom
Engine Component Improvement Office
NASA - Lewis Research Center, 21000 Brookpark Rd., Cleveland, Ohio 44135

16. Abstract

The JT9D-70/59 high pressure turbine active clearance control system was modified to provide further reduction of blade tip clearance when the system is activated during cruise operation. Engine testing was conducted to determine the effect on performance and deterioration. Rig testing was conducted to generate basic heat transfer data on the impingement cooling arrangement used, and to verify the mechanical functioning of the system.

The modification included increasing the flow capacity and air impingement effectiveness of the cooling air manifold to augment turbine case shrinkage capability, and modification of the turbine outer air seal support structure to increase responsiveness of the seal clearance to case shrinkage.

Simulated altitude engine testing indicated a significant improvement in specific fuel consumption with the modified system. A 1000 cycle engine endurance test showed no unusual wear or performance deterioiration effects on the engine or the clearance control system. Rig tests indicated that the air impingement and seal support configurations used in the engine tests are near optimum.

17. Key Words (Suggested by Author(s))	18. Distribution Statement
JT9D-70/59 Engine High-Pressure Turbine Active Clearance Control Blade Tip Leakage Reduction Specific Fuel Consumption Improvement	

19. Security Classif. (of this report)	20. Security Classif. (of this page)	21. No. of Pages	22. Price*
UNCLASSIFIED	UNCLASSIFIED	59	

* For sale by the National Technical Information Service, Springfield, Virginia 22161

FOREWORD

The development and demonstration effort described in this report was conducted by the Commercial Products Division of Pratt & Whitney Aircraft Group, United Technologies Corporation, under NASA Contract NAS3-20630. Mr. J. A. Ziemianski and Mr. T. N. Strom of the NASA-Lewis Research Center were the Project Manager and Project Engineer respectively for the contract.

This report was prepared by Mr. William O. Gaffin, Pratt & Whitney Aircraft Program Manager with the assistance of Messrs. Frederick D. Havens and Craig S. Vickery. The technical data presented herein was compiled with the cooperation of a wide segment of Engineering personnel. This report has been assigned the Commercial Products Division, Pratt & Whitney Aircraft Group Internal Report Number PWA-5513-87C.

TABLE OF CONTENTS

Section	Title	Page
1.0	Summary	1
2.0	Introduction	2
3.0	Design and Fabrication	4
4.0	Testing	7
	4.1 Altitude Performance Test	7
	4.1.1 Test Facility	7
	4.1.2 Test Procedure	9
	4.2 Performance Deterioration Test	10
	4.2.1 Test Facility	10
	4.2.2 Test Procedure	12
	4.3 Blowing Rig Test	15
	4.3.1 Rig Description	15
	4.3.2 Test Facility	21
	4.3.3 Test Procedure	21
	4.4 Slippage Rig Test	22
	4.4.1 Rig Description	22
	4.4.2 Test Facility	23
	4.4.3 Test Procedure	26
5.0	Results	27
	5.1 Altitude Performance Test	27
	5.2 Performance Deterioration Test	31
	5.3 Blowing Rig Test	32
	5.4 Slippage Rig Test	44
	5.5 Economic Evaluation	44
6.0	Concluding Remarks	48
APPENDIX A	Product Assurance	49
APPENDIX B	List of Abbreviations and Symbols	53
REFERENCE		54

LIST OF ILLUSTRATIONS

Number	Title	Page
3-1	Area of the JT9D-59/70 Engine Affected by the Active Clearance Control System	5
3-2	Comparison of Early Production and Improved Active Clearance Control Systems	6
4-1	X-217 Stand	7
4-2	HPT Case Thermocouple Locations.	9
4-3	JT9D-70/59 Experimental Engine X-622-12	11
4-4	Deterioration Test Cycle #1	13
4-5	Deterioration Test Cycle #2	14
4-6	Deterioration Test Cycle #3	15
4-7	Blowing Rig Test Section	16
4-8	Improved ACC Region Simulated by Blowing Rig	16
4-9	Blowing Rig Without Insulation Installed	19
4-10	Schematic Layout of Blowing Rig Test Set-up	20
4-11	Location of Thermocouples In the U-shaped Flange	21
4-12	Schematic Diagram of Slippage Rig	23
4-13	Slippage Rig	24
4-14	Slippage Rig Thermocouple and Dial Indicator Locations	25
5-1	TSFC vs Clearance Reduction at 90 Percent Maximum Cruise Power	28
5-2	TSFC vs HPT Case Temperature Reduction	29
5-3	Improvement in TSFC Cruise Thrust Relative to Early Production Engines	30

LIST OF ILLUSTRATIONS (Continued)

Number	Title	Page
5-4	Relative Heat Transfer Coefficient Versus Relative Cooling Airflow Results for Bolted Flange	33
5-5	Relative Heat Transfer Coefficient Versus Relative Cooling Airflow Results for Bolted Flange	33
5-6	Relative Heat Transfer Coefficient Versus Relative Cooling Airflow Results for Non-Bolted Flange	34
5-7	Relative Heat Transfer Coefficient Versus Relative Cooling Airflow Results for Non-Bolted Flange	34
5-8	Effect of Varying Hole Diameter on the Heat Transfer Effectiveness for the Bolted Side	36
5-9	Effect of Varying the Number of Holes on the Heat Transfer Effectiveness for the Non-Bolted Side	37
5-10	Effect of Varying Impingement Distance on the Heat Transfer Effectiveness for the Non-Bolted Side	38
5-11	Effect of Hole Location on the Heat Transfer Effectiveness for the Non-Bolted Side	39
5-12	Effect of Varying Impingement Angle on the Heat Transfer Effectiveness for the Non-Bolted Side	40
5-13	Effect of Varying the Number of Holes on the Heat Transfer Effectiveness for the Non-Bolted Side	41
5-14	Effect of Varying the Number of Holes on the Heat Transfer Effectiveness for the Bolted Side	42

LIST OF TABLES

Table	Title	Page
4-1	Instrumentation List for Performance Test of X-620-12	8
4-2	Instrumentation List for Performance Deterioration Test of X-622-12	12
4-3	Blowing Rig Impingement Geometries	18
4-4	Blowing Rig Test Instrumentation	20
4-5	Blowing Rig Test Points	22
5-1	Case Temperature Reduction and Clearance Reduction X-620-12 Engine	30
5-2	TSFC Reduction X-620-12 Engine	31
5-3	TSFC Reductions in X-622-12 Engine Deterioration Test	32
5-4	Slippage Rig Test Results	44
5-5	Predicted Engine Effects, JT9D-70/59 Engines	45
5-6	Airline Cost Evaluation	46
5-7	Fuel Saving Evaluation, World Fleet of 747 and DC10-40 Airplanes	47

1.0 SUMMARY

The objective of the JT9D-70/59 Improved High Pressure Turbine Active Clearance Control (hereinafter referred to as the improved ACC) Program was to demonstrate the thrust specific fuel consumption (TSFC) improvement of the concept and its performance deterioration characteristics. Preliminary analysis during the feasibility studies predicted 0.9 percent TSFC improvement of the concept relative to the early production active clearance control system at average cruise conditions.

To accomplish this improvement, the existing active clearance control system was re-designed to increase its flow capacity and impingement cooling effectiveness, and the high pressure turbine case and turbine outer airseal support assembly was modified to increase the responsiveness of that assembly to the active clearance control cooling air.

A simulated altitude test of an experimental JT9D-70/59 engine with the improved ACC system was conducted to determine its cruise performance improvement capability. This test was run by turning ACC cooling air "off" and "on" with gradually increasing amounts of cooling airflow to find the point at which no further performance improvement was obtained. A second engine with the improved ACC was subjected to a 1000 cycle sea level endurance test to evaluate the durability of the improved ACC system and its effects, if any, on engine performance deterioration characteristics. Rig tests were conducted to check the operation of the selected cooling pipe and seal support structure configurations, and to confirm the design capabilities of the configuration used in the engine tests.

A cruise TSFC improvement potential of 0.65 percent was demonstrated. This value is less than the predicted 0.9 percent because the turbine blade tip clearance available for closure with the improved ACC system apparently is less than earlier estimates. The system showed no unusual wear or deterioration effects in the 1000 cycle endurance tests, and the engine performance deterioration characteristics were not affected by the modification.

The airline "new buy" payback period for the concept will increase slightly over the ECI Feasibility Analysis evaluation because the performance improvement was less than the original prediction. However, the new buy payback period is still well within the acceptable limit (6 years), so the number of engines that will be affected by the concept should be unchanged. Consequently, the cumulative fuel saving will be reduced only by the ratio of demonstrated to predicted TSFC improvement, which results in an estimate of 1279 million liters (338 million gallons) saved.

2.0 INTRODUCTION

National energy demand has outpaced domestic supply, creating an increased U.S. dependence on foreign oil. This increased dependence was dramatized by the OPEC oil embargo in the winter of 1973-74. In addition, the embargo triggered a rapid rise in the cost of fuel which, along with the potential of further increases, brought about a changing economic circumstance with regard to the use of energy. These events, of course, were felt in the air transport industry as well as other forms of transportation. As a result of these experiences, the government, with the support of the aviation industry, has initiated programs aimed at both the supply (sources) and demand (consumption) aspects of the problem. The supply problem is being investigated by looking at increasing fuel availability from such sources as coal and oil shale. An approach to the demand aspect of the problem is to evolve new technology for commercial aircraft propulsion systems which will permit development of a more energy efficient turbofan or the use of a different propulsive cycle such as a turboprop. Although studies have indicated large reductions in fuel usage are possible (e.g., 15 to 40 percent), the fuel savings impact of developing and introducing into service a new turbofan or turboprop engine would not be significant for at least ten to fifteen years. In the short term, the only practical propulsion approach is to improve the fuel efficiency of current engines. Examination of this approach has indicated that a five percent fuel reduction goal, starting in the 1980-82 time period, is feasible. Inasmuch as commercial aircraft in the free world are using fuel at a rate in excess of 80 billion liters of fuel per year, even five percent represents significant fuel savings.

Since a major portion of the present commercial aircraft fleet is powered by the JT8D and JT9D engines, NASA is sponsoring a program whose objective is to reduce the fuel consumption of these engines. This program, called the Engine Component Improvement (ECI) program, has two main parts, performance improvement and engine diagnostics. The engine diagnostics program, which is not reported herein, is aimed at identifying the sources and causes of engine deterioration. The performance improvement (PI) program is intended to identify and evaluate the concepts which are technically and economically viable for the 1980-82 time period, and then develop and demonstrate these concepts through ground and flight tests. The PI program is being conducted by Pratt & Whitney Aircraft under NASA contract NAS3-20630. Eight promising concepts were identified from a list of over one hundred for further work and development. A report on the ranking of these concepts is contained in the Task I Feasibility Analysis (ref. 1). The contracted development and demonstration effort on two of the eight concepts have been completed. The first was the JT8D Revised High Pressure Turbine Cooling and Outer Air Seal concept, which is described in a separate document. The second is the JT9D-70/59 Improved High Pressure Turbine Active Clearance Control concept, which is the subject of this report.

The improved ACC concept improves the cruise TSFC of the engine by further reducing high pressure turbine (HPT) blade tip clearance as compared to the active clearance control system which was introduced in the early JT9D-70/59 production engines. The reduced blade tip clearance results in less leakage past the blade tips and an increase in turbine efficiency. The effort discussed in this report included completion of the design of the improved system, procurement of test hardware, and rig and engine testing.

3.0 DESIGN AND FABRICATION

The blade tip clearances in the HPT section of the JT9D engine vary during engine operation, becoming larger than desirable at cruise conditions. Large clearances allow leakage past the HPT blade airfoil tips, resulting in a loss in turbine efficiency and an increase in fuel consumption. Based on field experience, the turbine tip clearances are set during engine build-up to avoid rubbing between the outer air seal and the blade tip during takeoff and engine transients, conditions at which the most critical combination of thermal transient and structural loading occur. The tip clearances decrease due to the differences in the radial growth rate of the rotor system and the case, which is caused by changing temperatures and centrifugal forces in the rotor system. The turbine blades are also susceptible to rubbing during airplane maneuver operation(s) such as takeoff, climb and landing due to inertial and aerodynamic loads. Setting the blade tip clearance to avoid rubs at these conditions results in a larger than desirable clearance at cruise conditions when the engine and flight path are stabilized. By cooling the HPT case to a lower temperature during cruise operation and causing it to contract, the blade tip clearances can be reduced, improving the turbine efficiency and fuel consumption.

An active clearance control system is used in the JT9D-70/59 series of engines to accomplish this reduction in blade tip clearance. The clearance control is automatically turned on at a predetermined altitude, and is shut off at an engine power level above maximum cruise and during transient and maneuver operation. The active clearance control system works by ducting cooling air from the fan through a supply system to pipes encircling the HPT case. The air impinges on the HPT case through holes in the pipes, cooling the case and causing it to contract. A valve in the supply line is used to turn the clearance control system on and off.

The active clearance control system used in early JT9D-70/59 production engines was designed with a single cooling air supply pipe from the fan to the cooling pipes. The cooling pipes were of round cross-section, completely encircling the HPT case. Cooling air was supplied to the pipes from a single location and distributed to the case via small holes in the pipes. The HPT case cooling was limited by the airflow capacity of this system. Engine tests, using an external high pressure air supply connected to this system, indicated that greater reductions in tip clearance and further improvements in TSFC were possible before encountering a blade tip rub.

An improved ACC system was designed to increase the amount of clearance reduction that could be achieved. Improvements over the early production system included: 1) an improved air delivery and distribution system featuring two cooling air supply pipes instead of only one, 2) "square" cooling air pipes of increased cross-sectional area

positioned closer to the turbine case flanges and rails, and 3) a modified high pressure turbine case and outer airseal support assembly that allows the HPT case to contract more freely. The area of modification is shown in Figure 3-1. A comparison of the early production active clearance control and the improved ACC is shown in Figure 3-2.

The cooling air pipes were changed from a round to a square shape to allow the cooling air pipes to be nested closer to the turbine case flanges and rails. Cooling air hole spacing, diameter, impingement angle, number of jets and distance from the flange surface also were changed to improve cooling effectiveness. The cooling hole area was also increased to increase the flow capacity and the cooling capability of the system.

As indicated above, the outer air seal support and its method of assembly to the turbine case were modified to increase the responsiveness of the outer air seal. This in turn permits better control of the turbine tip clearance, which is determined by the radial movement of the outer air seal.

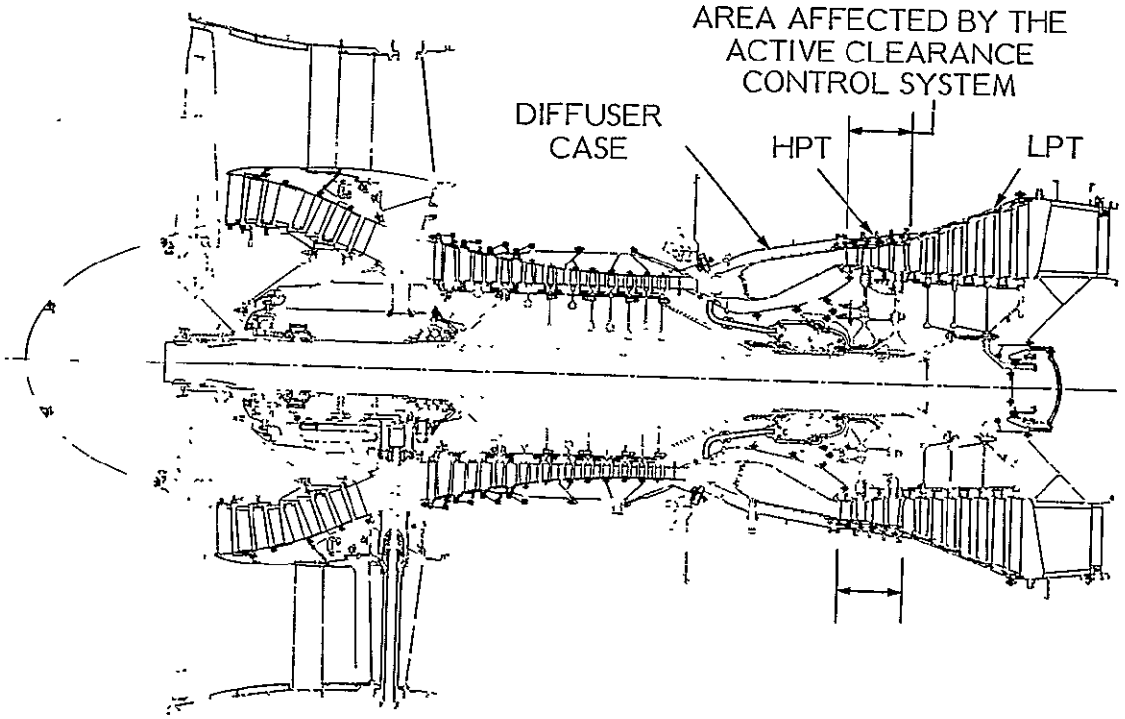

Figure 3-1 Area of the JT9D-59/70 Engine Affected by the Active Clearance Control System.

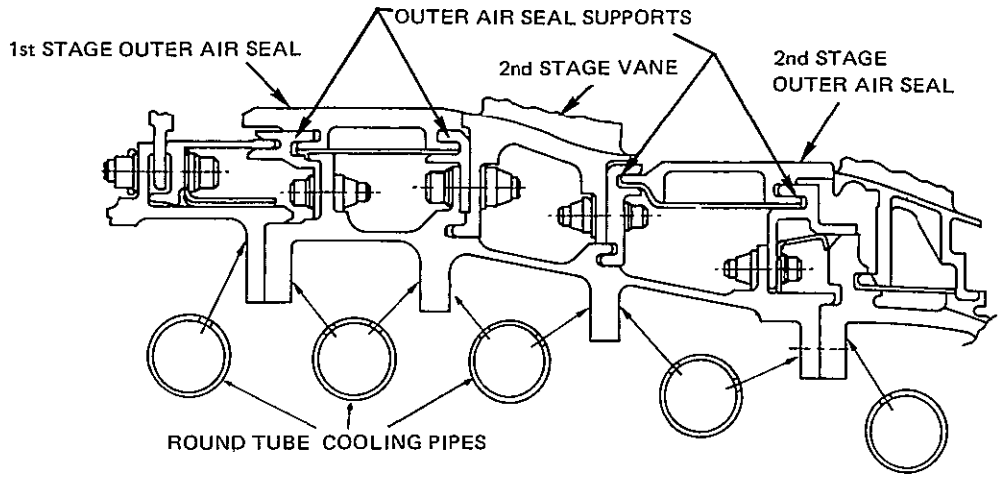

(A) EARLY PRODUCTION ACTIVE CLEARANCE CONTROL

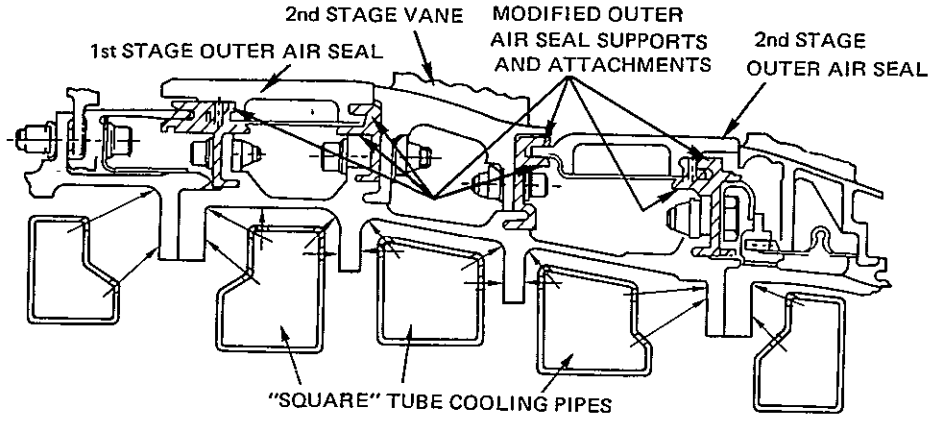

(B) IMPROVED ACTIVE CLEARANCE CONTROL

Figure 3-2 Comparison of Early Production and Improved Active Clearance Control Systems

4.0 TESTING

4.1 Simulated Altitude Performance Test

The test objective was to experimentally determine the engine cruise TSFC improvement provided by the improved ACC configuration. The test was conducted at a simulated altitude of 10,670 m (35,000 ft) above sea level at Mach 0.84. These conditions simulate cruise flight conditions that the engine would encounter in actual service.

4.1.1 Test Facility

The test vehicle for the simulated altitude testing was JT9D-70/59 experimental engine X-620-12. The test facility for this test was X-217 stand, shown in Figure 4-1. X-217 stand is the largest full scale engine stand in the Willgoos Laboratory, sized specifically to test the largest P&WA engines at simulated altitudes from 6,100 to 14,600 m (20,000 to 48,000 ft) at flight Mach numbers of 0.6 to 1.0. The stand consists of an enclosed test cell and an adjacent control room. The cell contains an altitude chamber within which a test engine is suspended from an overhead mounting system which incorporates a 1.1 x 10^5 N (25,000 lbf) thrust measuring system.

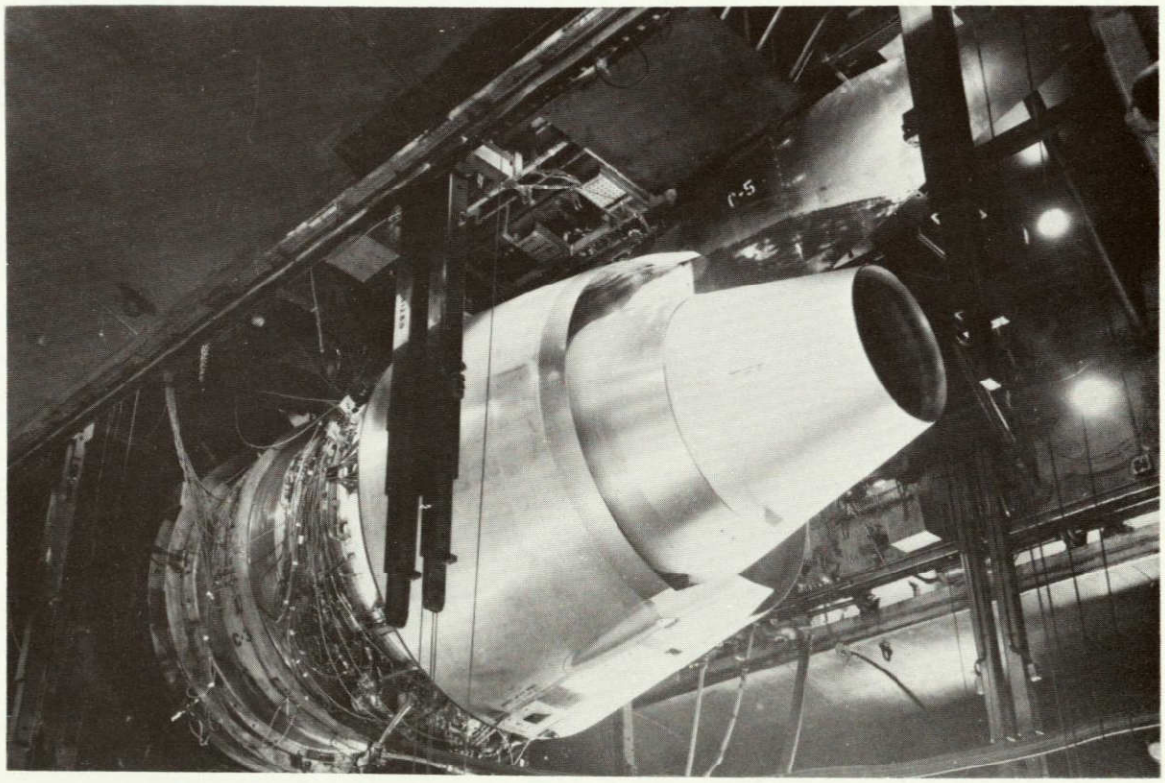

Figure 4-1 X-217 Stand

Gaspath performance and stand instrumentation used for X-620-12 engine in X-217 stand is shown in Table 4-1. Figure 4-2 shows the location of the 64 thermocouples installed on the high pressure turbine case used to measure case temperature reductions during operation of the ACC system.

TABLE 4-1

SIMULATED ALTITUDE PERFORMANCE TEST INSTRUMENTATION
X-620-12 ENGINE

Parameter	Minimum Number of Sensors
Atmospheric Pressure	1
Fan Inlet Total Pressure	8
Fan Inlet Static Pressure	8
LPC Exit Total Pressure	1
LPC Exit Static Pressure	1
Fan Inlet Total Pressure	4 Rakes/5 Per Rake
Combustor Pressure	1
Compressor Exit Total Temperature	4 Rakes/3 Per Rake
Turbine Exhaust Total Pressure	1 Manifolded (Production Instrumentation)
Fan Duct Total Pressure	1 Manifolded
Fan Exit Total Pressure	8 Rakes/8 Per Rake
Inlet Total Temperature	36
LPC Exit Total Temperature	4 Rakes/5 Per Rake
HPC Exit Total Temperature	1 Probe (In Borescope Hole)
HPC Exit Total Temperature	4 Rakes/3 Per Rake
Turbine Exhaust Total Temperature	6
Fan Exit Total Temperature	8 Rakes/8 Per Rake
Low Pressure Rotor Speed	1
High Pressure Rotor Speed	1
Fuel Flow	2
Fuel Temperature	2
Net Thrust	2
Stator Vane Angle	(Inlet Guide Vanes, 5TH, 6TH, and 7TH Stages)
Dew Point	1
Venturi Total Temperature	32
Venturi Static Temperature	5
Plenum Static Pressure	3
Ejector Pressure	1
HPT Case Temperature	64

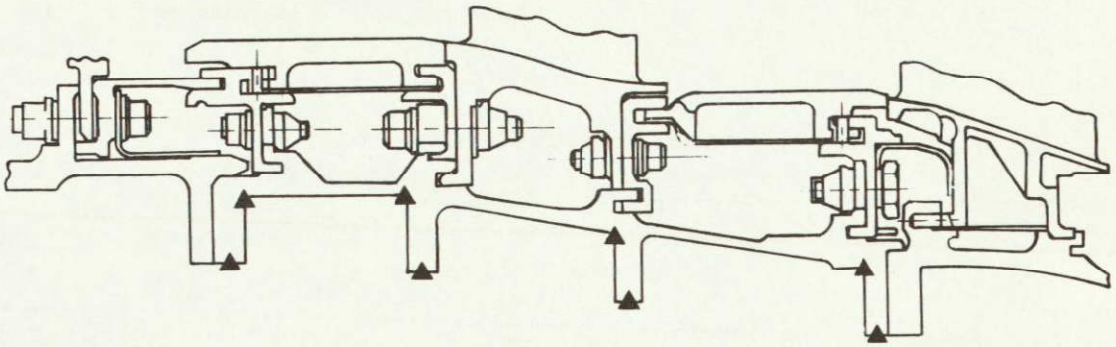

Figure 4-2 *HPT Case Thermocouple Locations. Thermocouples are located around the HPT case at 0°, 35°, 90°, 125°, 180°, 215°, 270°, 305°*

4.1.2 Test Procedure

The test engine was mounted in X-217 stand with the improved ACC hardware installed. An orifice plate was installed in the air ducts which deliver air to the ACC system. The orifice plate had been sized to limit the ACC cooling airflow to achieve approximately a 103°C (185°F) temperature reduction in the HPT case O.D. at 75 percent maximum cruise power. The engine was started and all instrumentation and recording equipment was checked for proper operation with the engine idling. The altitude chamber was then brought to 10,700 m (35,000 ft) Mach 0.84 simulated conditions.

Engine performance data points were taken at eight evenly spaced thrust levels with the ACC system off. These thrust levels were taken in decreasing sequence from maximum climb power to 60 percent maximum cruise power.

The ACC system was then actuated and ten evenly spaced data points were taken in decreasing sequence from maximum cruise thrust to 60 percent of maximum cruise thrust. The ACC system was turned off and data was taken at four thrust levels decreasing from maximum climb to 65 percent maximum cruise thrust to check for deterioration of the engine performance.

The engine was shut down and orifices sized to obtain a 111°C (200°F) case temperature reduction were installed in the air delivery ducts. The engine was started, the ACC system was activated, and

data was taken at ten evenly spaced thrust points from maximum cruise thrust to 60 percent maximum cruise thrust. The ACC system was shut off and a five point performance deterioration check was taken at decreasing thrust levels from maximum climb to 65 percent maximum cruise.

Larger orifice plates were installed to obtain a 122°C (220°F) temperature reduction. The engine was started and the ACC system was activated. Ten evenly spaced data points were taken from maximum cruise to 63 percent maximum cruise. The ACC system was then turned off and another five point deterioration check was made.

For the final calibration orifices were installed to obtain a 133°C (240°F) temperature reduction on the HPT case. Eight evenly spaced data points were taken from maximum cruise to 65 percent maximum cruise with the ACC system on. The ACC system was then turned off and an eleven point performance deterioration check made from maximum climb to 60 percent maximum cruise.

4.2 Deterioration Test

The objective of the deterioration test was to determine the performance deterioration of an engine with the improved ACC system relative to an engine with the early production round pipe ACC configuration after a 1000 cycle endurance test.

4.2.1 Test Facility

The test vehicle for this test was JT9D-70/59 experimental engine X-622-12, shown in Figure 4-3. The test facility for this test was X-8 stand. This stand is a gas turbine engine test facility located in the main test complex designed to test large turbofan and turbojet development engines at static sea level conditions. The stand, a reinforced concrete structure, is divided into two sections by a structural steel bulkhead. The bulkhead is provided with sectional hinged doors to permit engine installation and removal, and two personnel doors. The rear section of the stand contains the test engine area and a portion of the exhaust ejector. Structural steel platforms which can be hydraulically lowered to install the engine are located approximately 3.5 m (11.5 ft) above the floor. Fixed platforms are provided above the engine for access to test instrumentation.

The control room is located adjacent to the test cell. Special cabling is provided from the test cell to the control room and an outside mobile van panel. This system provides for connecting special instrumentation such as an automatic plotter, vibration meters, pressure transducers, strain gages, closed circuit television, fuel flows, and communications. Instrumentation can be installed on the engine prior to delivery to the test stand, and connected to panels provided for this purpose on the flexible mounting structure.

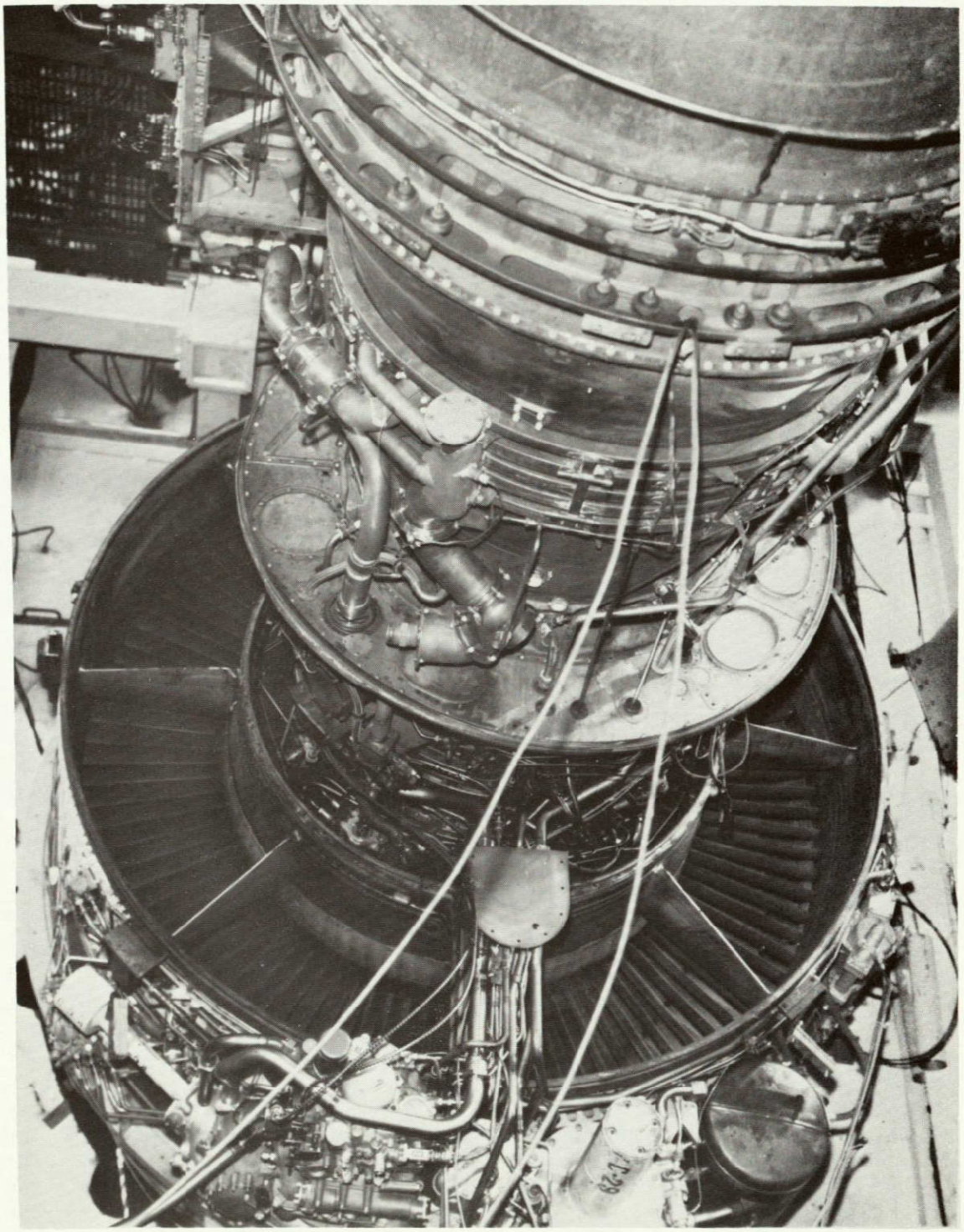

Figure 4-3 JT9D-70/59 Experimental Engine X-622-12

The gaspath performance and stand instrumentation used for X-622-12 engine in X-8 stand is shown in Table 4-2.

TABLE 4-2

DETERIORATION TEST INSTRUMENTATION
X-622-12 ENGINE

Parameter	Minimum Number of Sensors
Atmospheric Pressure	1
Engine Inlet Total Pressure	8
Engine Inlet Static Pressure	8
Burner Pressure	1
Turbine Exhaust Total Temperature	6 Manifolded (Production Instrumentation)
Ambient Temperature	1
Compressor Exit Total Temperature	2 Probes (In Borescope Holes)
Turbine Exit Total Temperature	6 Rakes with Averaging Harness (Production Instrumentation)
Low Pressure Rotor Speed	1
High Pressure Rotor Speed	1
Fuel Flow	2
Fuel Temperature	2
HPC Stator Vane Angle	2
Net Thrust	2
Relative humidity	1

4.2.2 Test Procedure

The test engine was mounted in the stand with the improved ACC system installed. The ACC system was connected to the test stand compressed air supply because the fan pressure ratio at sea level conditions is not high enough to produce the necessary flow to the ACC system. All instrumentation was installed and the thrust meter calibrated. The engine was started and a fuel sample taken for analysis while the engine was idling.

A baseline performance calibration was run at six thrust levels between 65 percent takeoff and full takeoff power with the ACC off and the station 3 bleed closed. A five point performance calibration was also run at thrust levels varying from 140,000 N to 98,000 N (32,000 to 22,000 pounds) with the ACC system "on" and "off" at each thrust level. This thrust range is equivalent to the corrected altitude cruise operating range.

After completion of the performance calibration runs the first endurance test cycle was begun with the ACC system "off". A test cycle consisting of flight idle, simulated reverse, ground idle, takeoff and a series of intermediate thrust levels was run 760 times. This cycle (#1) is given in Figure 4-4. At the end of every 100 cycles during the 15 step reduction in high pressure rotor speed, engine data was recorded for calculation of engine performance. At no time during this series of cycles was the ACC turned "on". A total of 63.3 hours was spent in the takeoff and simulated reverse modes.

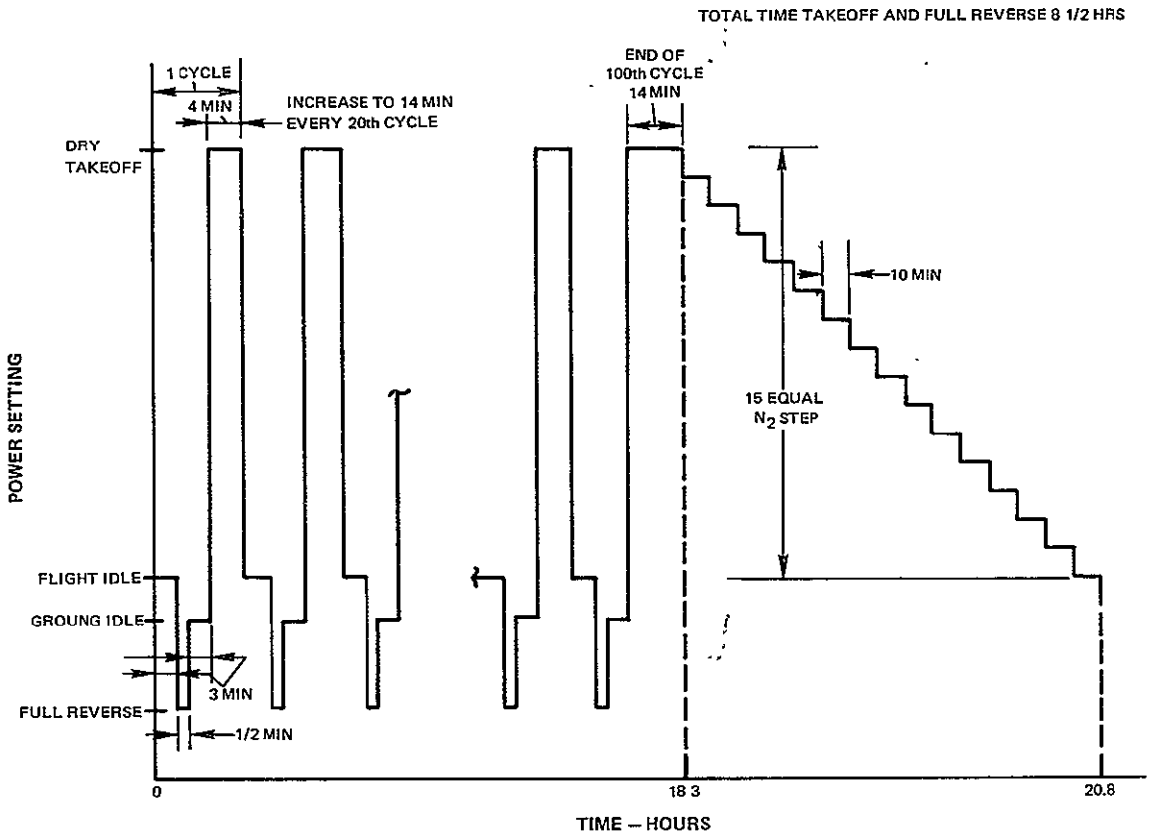

Figure 4-4 Deterioration Test Cycle #1

At this point the endurance test cycles were changed to test cycles #2 and #3. Testing continued for another 114 hours, generating another 228 cycles for a combined total of 988 cycles. The 114 hours of cyclic operation was composed of 15 runs through the cycle #2 shown in Figure 4-5 and four runs through the cycle #3 shown in Figure 4-6. These cycles consist of the same engine power settings as in the first type of cyclic testing, but for different lengths of time. A total of 12.5 hours was spent at takeoff and simulated full reverse operation during this cyclic testing.

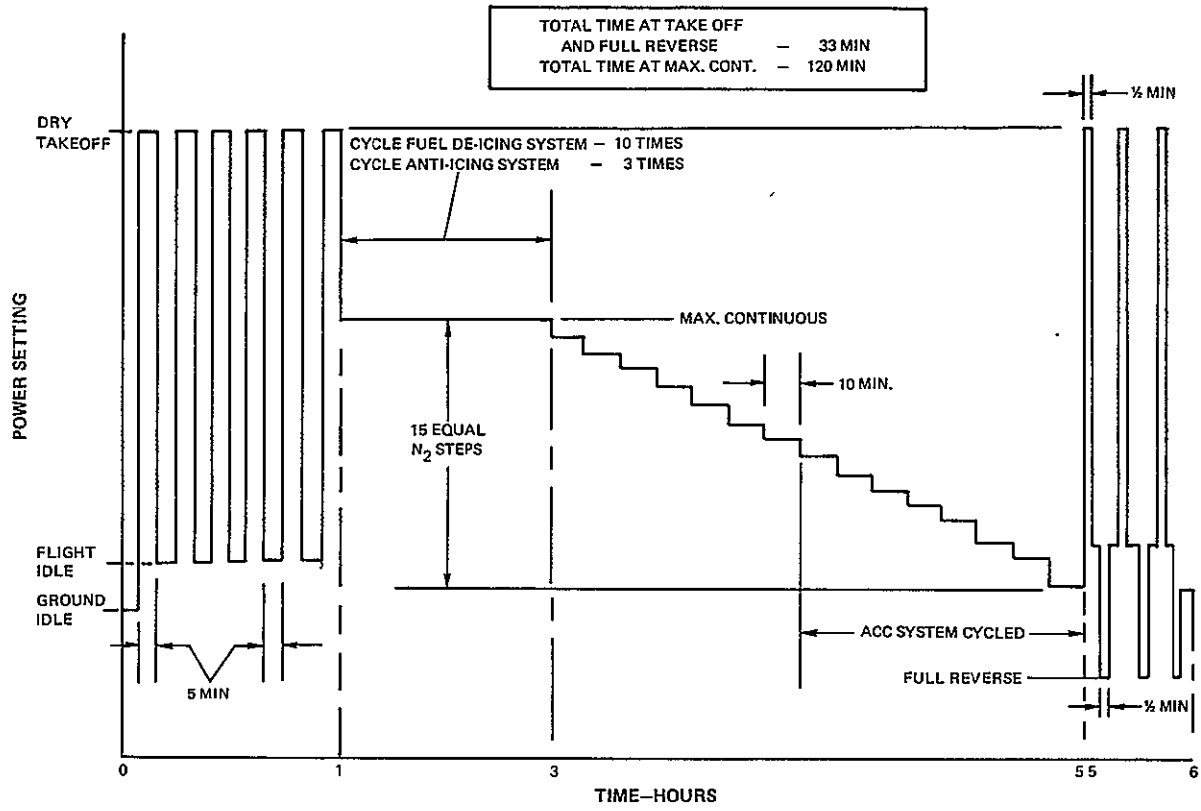

Figure 4-5 Deterioration Test Cycle #2

Cyclic testing of the ACC system was conducted during test cycles #2 and #3. While running the eighth through fifteenth steps of the 15 step reduction in high pressure rotor speed of test cycle #2, the ACC system was continuously cycled between "off" and "on" at 45 second intervals. During test cycle #3 the ACC system was continuously cycled between "off" and "on" every 45 seconds during all 15 rotor speed steps. 1007 cycles of ACC operation were accumulated during this portion of the endurance test.

After the endurance testing and cycling of the ACC was completed, a performance calibration was repeated at six thrust levels varying from 140,000 N to 98,000 N (32,000 to 22,000 pounds) with the ACC "on" and "off" at each thrust level.

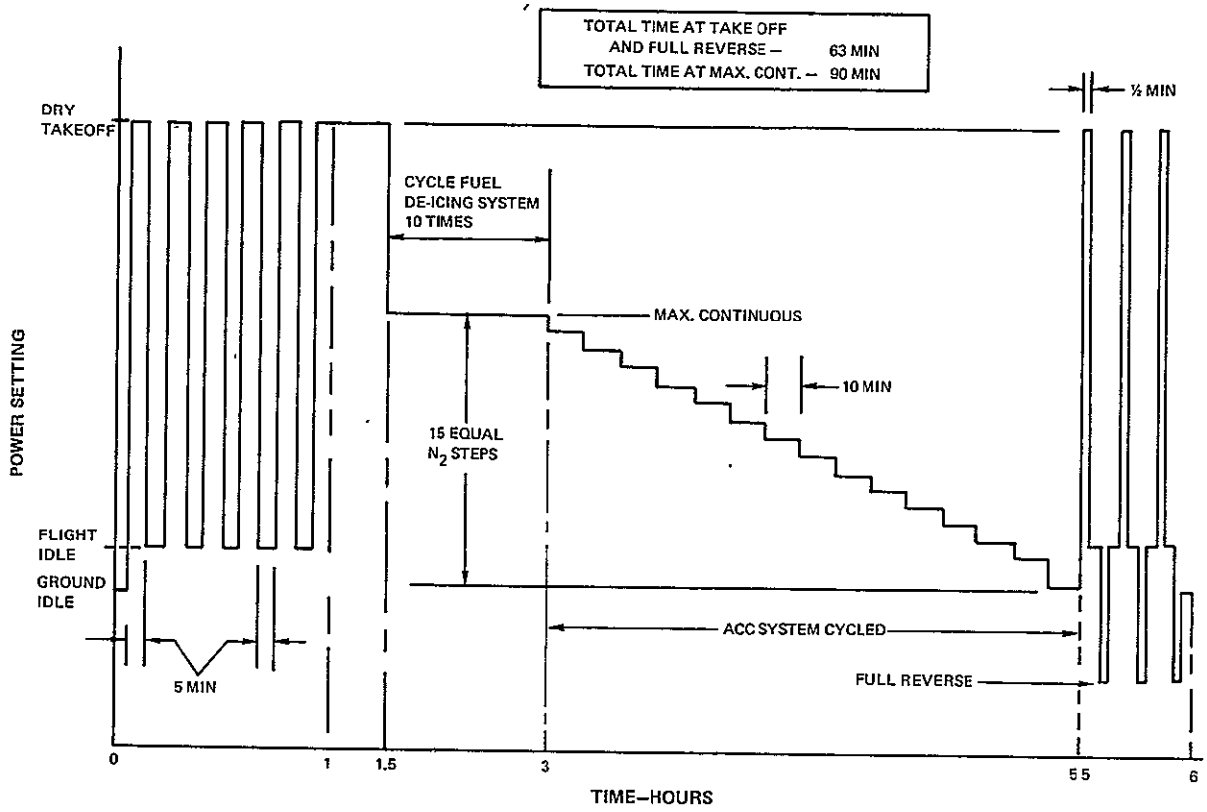

Figure 4-6 Deterioration Test Cycle #3

4.3. Blowing Rig Test

The objective of this test was to obtain basic heat transfer data with an impingement cooling configuration that simulates the improved ACC system. Sixteen cooling hole configurations were tested in the blowing rig with a variety of heat inputs and cooling air flows.

4.3.1 Rig Description

The blowing rig is a twice actual size metal scale model of an ACC cooling air impingement pipe and the "U" shaped flange area. The rig is designed to simulate the heat transfer characteristics of one cooling pipe in the improved ACC system. The rig was scaled twice actual size to minimize instrumentation installation problems and to make fabrication and assembly easier. The simulated flange and impingement tube is shown in Figure 4-7. The section of the engine which the blowing rig was designed to simulate is shown in Figure 4-8.

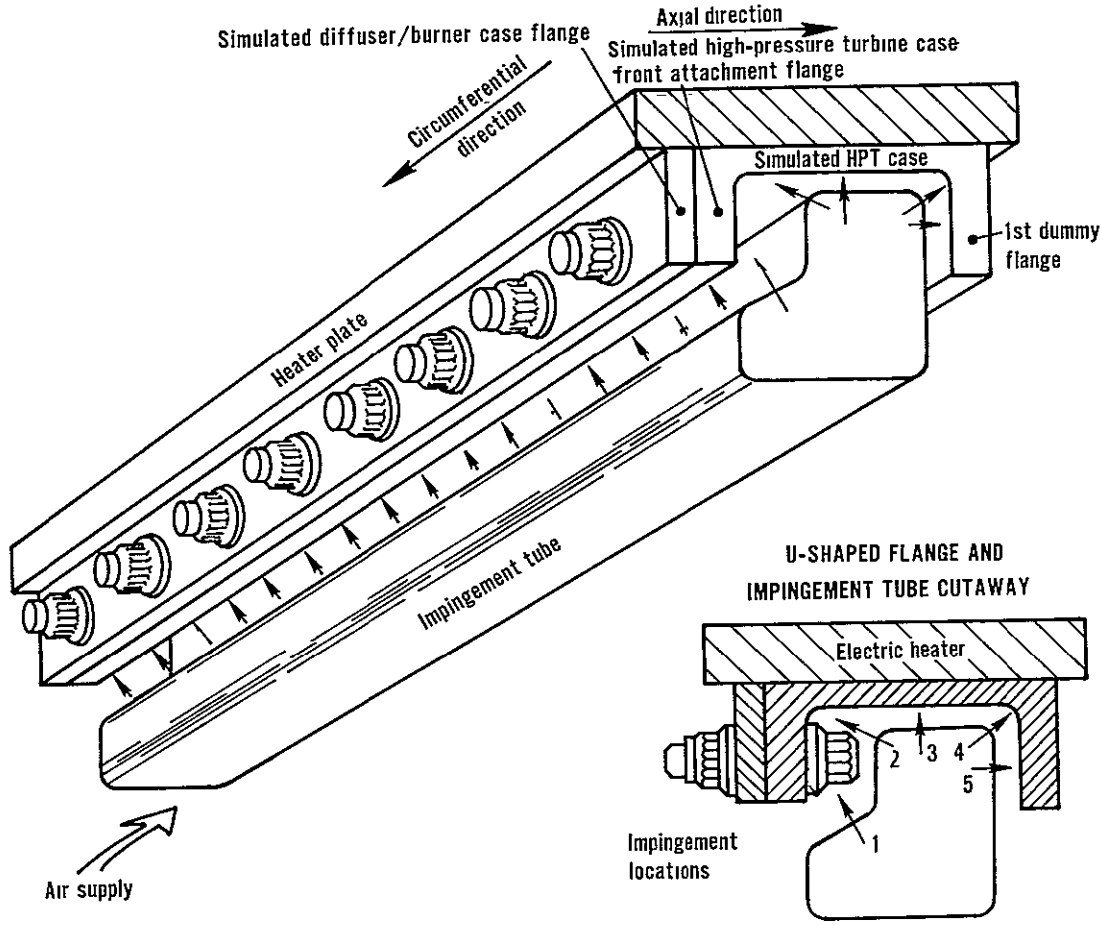

Figure 4-7 Blowing Rig Test Section

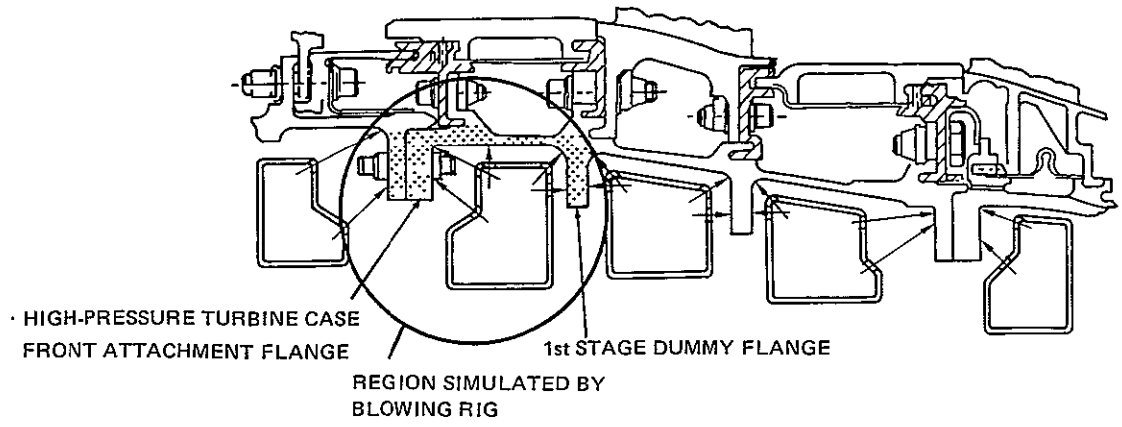

Figure 4-8 . Improved ACC Region Simulated by Blowing Rig

Six electric heaters, each with a maximum power output of 400 watts, were used to simulate the engine heat that the HPT case flange would experience in actual use. Three powerstats were used to individually regulate the power output of each end heater and the cluster of four central heaters. The end heaters were independantly controlled so that they could be set to eliminate end effects.

The rig cooling air impingement pipe was designed with a total of 16 test impingement geometries, as shown in Table 4-3. The cooling pipe is of the same cross-section geometry as the engine hardware. The impingement tubes were formed in two halves from sheet metal and were seam welded together. A long entrance section was provided (approximately 5 hydraulic diameters) to minimize entrance and end effects. An exhaust pipe was attached to the downstream end and flow control valves attached to the inlet and exhaust of the rig so that a flow split could be maintained between the impingement air and exhaust air. This flow split was created to simulate the flow split that occurs in a representative center section of the engine hardware. Two support plates were welded to the bottom of the impingement tube for positioning the tube relative to the "U" shaped flange section. Seven "dummy" bolts, fabricated from standard aircraft bolts, were attached to one side of the "U" shaped channel to simulate the engine bolts which hold two of the HPT case flanges together. The "U" shaped channel was fabricated from a block of 316 stainless steel material, because its heat transfer characteristics simulate the actual engine hardware.

The "U" shaped flanged section is bolted to a base plate by two support brackets at each end of the flange section. A plate covers the gap between the "U" shaped channel and impingement tube at each end of the channel to prevent flow along the length of the cooling pipes, which is equivalent to circumferential flow in an engine. Circumferential flow does not occur in an engine because of the continuous nature of the cooling pipes. A photograph of the rig is shown in Figure 4-9.

Fiberglass insulated chromel-alumel thermocouples were used to measure the metal temperature of the rig, as shown in Figure 4-10. The thermocouples were installed in slots and the junctions heliarc welded in place so that they were approximately 0.051 - 0.127 mm (0.002 - 0.005 in) below the surface. Batch calibrations of the wires were made to ensure a thermocouple wire accuracy of $\pm 0.3^{o}C$ ($0.5^{o}F$). Plenum air thermocouples were also installed in the impingement tube insert. These thermocouples were of the same type mentioned above. The junctions were made with a wire-to-diameter ratio of approximately 40/1 to ensure minimum conduction effects. All thermocouples were connected to a multi-pole switch and a precision indicator. The readout accuracy of this system is $\pm 0.3^{o}C$ ($0.5^{o}F$).

TABLE 4-3

BLOWING RIG IMPINGEMENT GEOMETRIES

Config. Number	Test Configuration Geometry Description	Number of Holes - Hole Diameter, mm (in.) Bolted Side Row-1	Bolted Side Row-2	Bolted Side Row-3	Non-Bolted Side Row-4	Non-Bolted Side Row-5	Non-Bolted Side Row-6	Percent Hole Area - Bolted Side
1	Prototype design hole size and spacing	21-2.34 (0.092)	11-2.36 (0.093)	20-1.93 (0.076)	20-1.93 (0.076)	20-1.93 (0.076)	-	53.4
2	Same as #1 except holes in rows 1 & 2 respaced circumferentially to be between bolts only	9-2.59 (0.102)	9-2.59 (0.102)	"	"	"	-	45.9
3	Same as #2 except hole diameter of rows 1 & 2 reduced 25%	9-1.93 (0.076)	9-1.93 (0.076)	"	"	"	-	35.9
4	Same as #2 except hole diameter of rows 1 & 2 increased 25%	9-3.25 (0.128)	9-3.25 (0.128)	"	"	"	-	55.0
5	Not used in test.							
6	Not used in test.							
7	Same as #1 except row 5 deleted and additional holes added to row 4 to maintain total flow	20-2.59 (0.102)	11-2.59 (0.102)	"	39-1.93 (0.076)	-	-	57.3
8	Same as #1 except row 4 deleted and additional holes added to row 5 to maintain total flow	"	"	"	-	39-1.93 (0.076)	-	57.3
9	Same as #1 except row 4 and 5 circumferential hole spacing increased 12% and total flow reduced correspondingly	"	"	"	18-1.93 (0.076)	18-1.93 (0.076)	-	58.9
10	Same as #1 except row 4 and 5 circumferential hole spacing decreased 13% and total flow increased correspondingly	"	"	"	23-1.93 (0.076)	23-1.93 (0.076)	-	54.0
11	Same as #1 except row 4 and 5 circumferential hole spacing increased 36% and total flow reduced correspondingly	"	"	"	15-1.93 (0.076)	15-1.93 (0.076)1	-	62.2
12	Same as #1 except row 4 and 5 circumferential hole spacing decreased 27% and total flow increased correspondingly	"	"	"	27-1.93 (0.076)	27-1.93 (0.076)	-	50.7
13	Determined by results of tests 1-12; perpendicular impingement	20-2.64 (0.104)	11-02.64 (0.104)	"	12-1.93 (0.076)	15-1.93 (0.076)	27-1.93 (0.076)	59.1
14	Determined by results of tests 1-13; bolted side versus unbolted side	18-1.93 (0.076)	18-1.93 (0.076)	"	15-2.59 (0.102)	15-2.59 (0.102)	-	41.8
15	Same as #1 except row #3 deleted	20-2.64 (0.104)	11-2.64 (0.104)	-	20-1.93 (0.076)	20-1.93 (0.076)	-	59.2
16	Determined by results of tests 1-15; change in impingement distance of test #10	20-2.64 (0.104)	11-2.64 (0.104)	20-1.93 (0.076)	23-1.93 (0.076)	23-1.93 (0.076)	-	54.8
17	Determined by results of tests 1-16; 1/2 of test #2	5-2.64 (0.104)	5-2.64 (0.104)	10-1.93 (0.076)	10-1.93 (0.076)	10-1.93 (0.076)	-	48.7
18	Round pipes, current in-service hole size and spacing	8-3.05 (0.120)	8-3.05 (0.120)	-	-	-	-	50.0

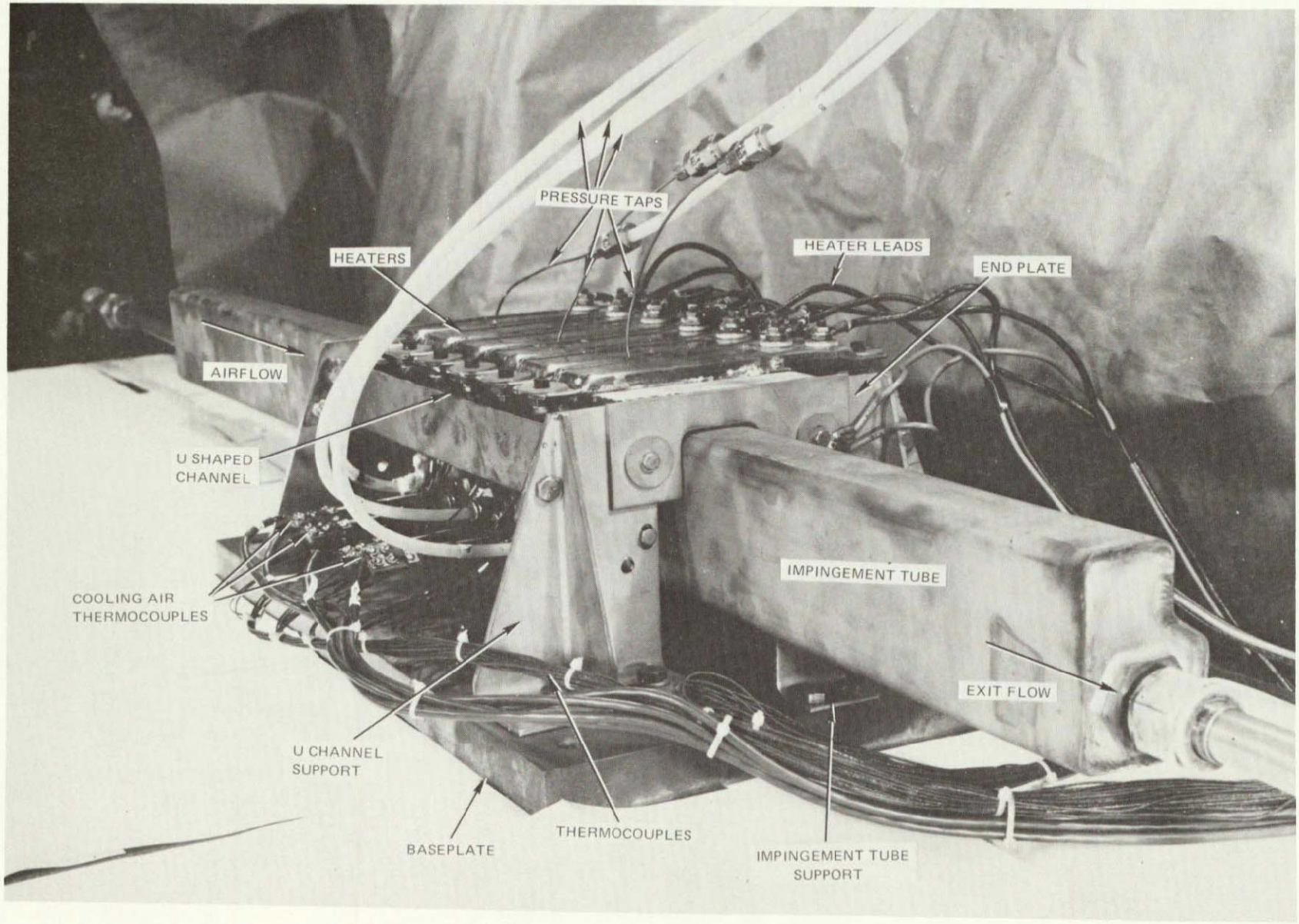

Figure 4-9 Blowing Rig Without Insulation Installed

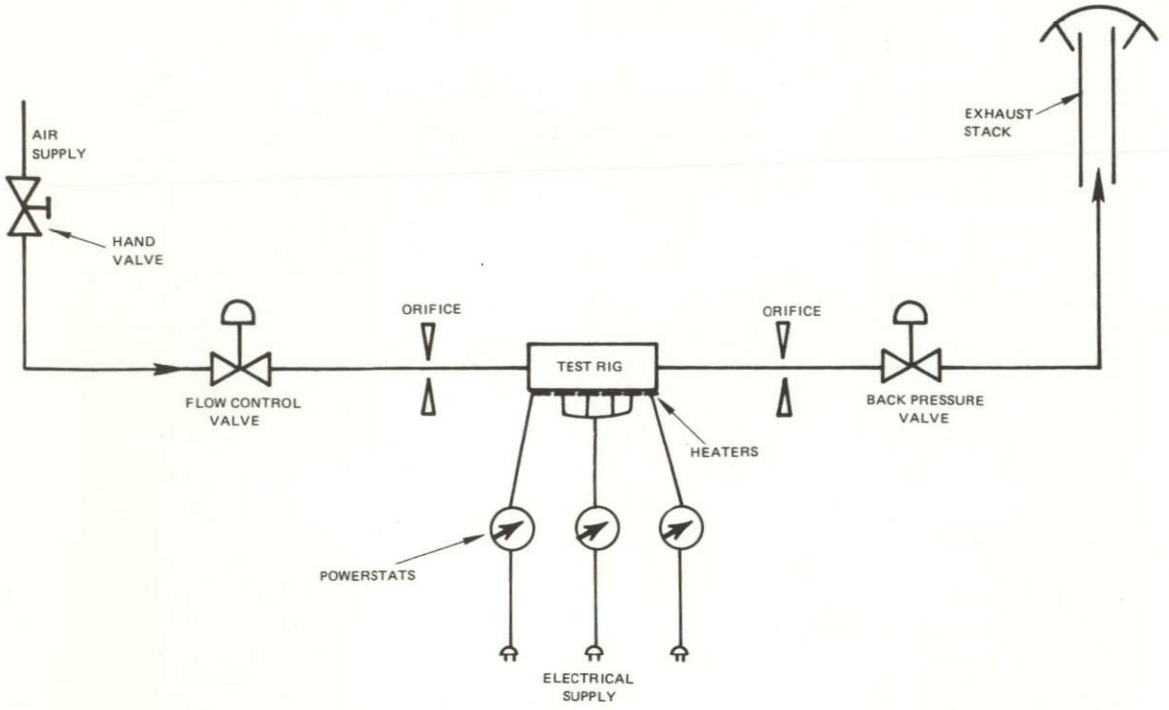

Figure 4-10 Schematic Layout of Blowing Rig Test Set-up

Static pressures were measured at several locations along the rig and within the impingement tube insert. Hypo tubing was connected from the pressure tap to a scanning valve system and then to a 0-1270 mm (0-50 in) of mercury digital pressure gauge. The accuracy of pressure measurements is $\pm$0.5 percent of full scale.

Flows were measured using standard orifice techniques. Several orifices were available to provide the required flow ranges. The accuracy of the flow measuring system is about $\pm$3 percent. A list of the instrumentation for the blowing rig is shown in Table 4-4.

TABLE 4-4

BLOWING RIG TEST INSTRUMENTATION

Parameter	Minimum Number of Sensors
Atmospheric Pressure	1
Upstream orifice pressure	1
Orifice pressure drop	1
Downstream orifice pressure	1
Orifice pressure drop	1
Cooling pipe total pressure	3
Cooling pipe discharge static pressure	3
Upstream orifice temperature	1
Downstream orifice temperature	1
Cooling air temperature	4
U-Flange metal temperature	40
Heater power	3

4.3.2 Test Facility

The test was conducted in X-917 stand in the Middletown test facility. The stand facilities consist of a compressed inlet air supply, an orifice system, and exhaust stack and valving system as diagrammed in Figure 4-11. The blowing rig was installed with an orifice on either side so the flow from the impingement holes could be determined. Three 110 volt 30 amp electrical circuits were used to supply power to the electrical heaters. The test facility has an air supply capacity of up to 1.4 Kg/s (3 lbm/s) and 6.9 x 10^5 Pa (100 psi). Electrical hookups, instrumentation, and other necessary hardware and equipment to perform this test were available in this facility.

4.3.3 Test Procedure

Fifteen square pipe configurations were tested in the blowing rig to determine the effect of varying hole size, hole spacing, striking distance, target points, and impingement angle relative to the configurations used in the engine tests. A round pipe was also tested to simulate the early production system. The configurations are identified and described in Table 4-3. The test conditions are listed in Table 4-5.

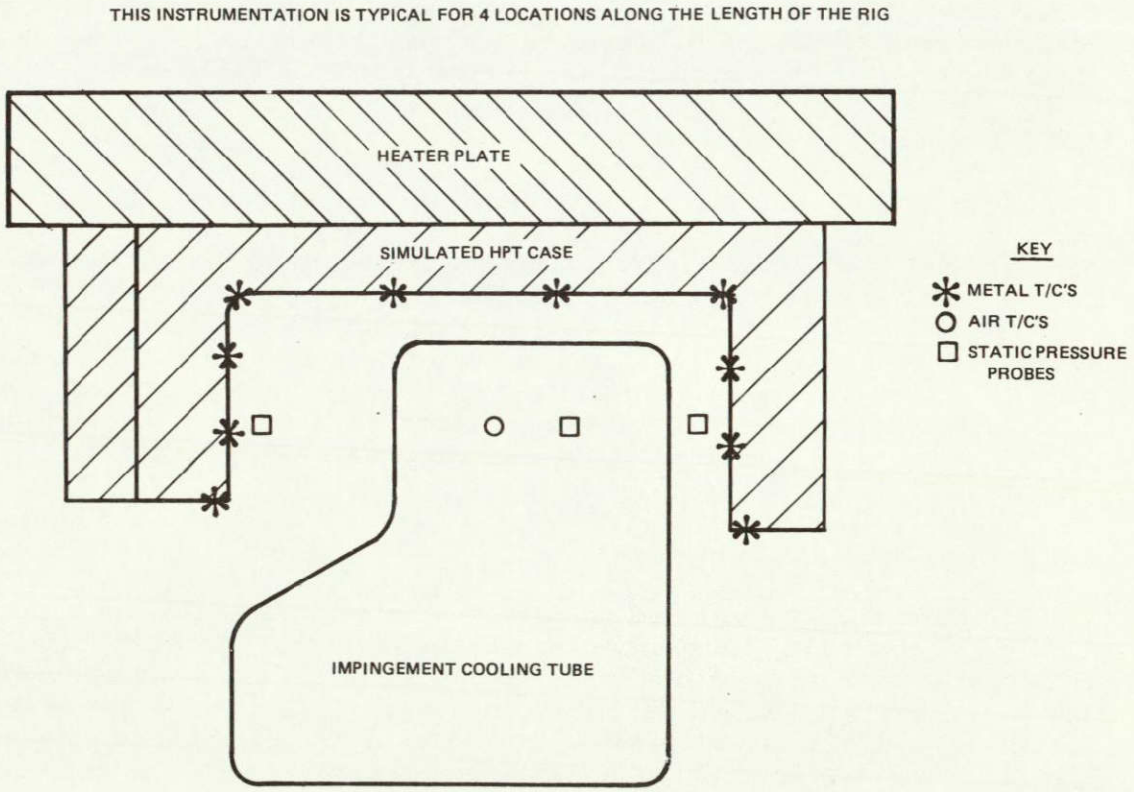

Figure 4-11 Location of Thermocouples In the U-shaped Flange

TABLE 4-5

BLOWING RIG TEST POINTS

Input Power (watts)			
End Heaters Each	Center Heaters Total	Total Heater Output	Impingement Pressure Ratio
83	333	500	1.1, 1.2, 1.3, 1.4, 1.5, 1.6
166	666	1000	1.1, 1.2, 1.3, 1.4, 1.5, 1.6
250	1000	1500	1.1, 1.2, 1.3, 1.4, 1.5, 1.6
300	1120	1720	1.1, 1.6

The hole rows are defined in Figure 4-7. Rows 1, 2 and 3 impinge on the bolted flange side of the rig, while rows 4 and 5 impinge on the non-bolted side. Row 6 was added on the non-bolted side of configuration 13 only. The hole patterns were varied independently on the two sides, and the flow split to the two sides was assumed proportional to the flow hole areas. The relative flow areas are indicated in the last column of Table 4-3.

After installation of each configuration in the rig, heater power was set, pipe airflow was set by controlling the impingement pressure ratio (the ratio of supply pipe pressure to atmospheric pressure), and case temperatures and other measurements were recorded after the temperature stabilized. Each configuration was tested at the four heat inputs and six impingement pressure ratios listed in Table 4-5.

4.4 Slippage Rig Test

The objective of the slippage rig test was to determine the optimum turbine case and seal support assembly for the improved ACC system. Several seal support configurations were tested by mounting them in a rig and heating them. The amount of case expansion measured at a given I.D. seal support temperature and the variation of expansion around the circumference of the case gave an indication of how each seal support configuration would respond to the active clearance control system in the engine. The rig was not expected to simulate the circularity of an operating engine, since pressure and bending loads were not imposed.

4.4.1 Rig Description

The slippage rig was designed to measure the case expansion as a function of temperature difference across the HPT seal and HPT case. A full scale HPT case with one seal support assembly and a pair of cooling air pipes was set up as shown in Figure 4-12. The HPT case was bolted to a LPT case to provide a realistic structural environment. The LPT case was mounted on a large support ring with the LPT case rear flange restrained radially. The inside of the assembly, except the seal support, was covered with insulation to minimize unwanted heat transfer effects.

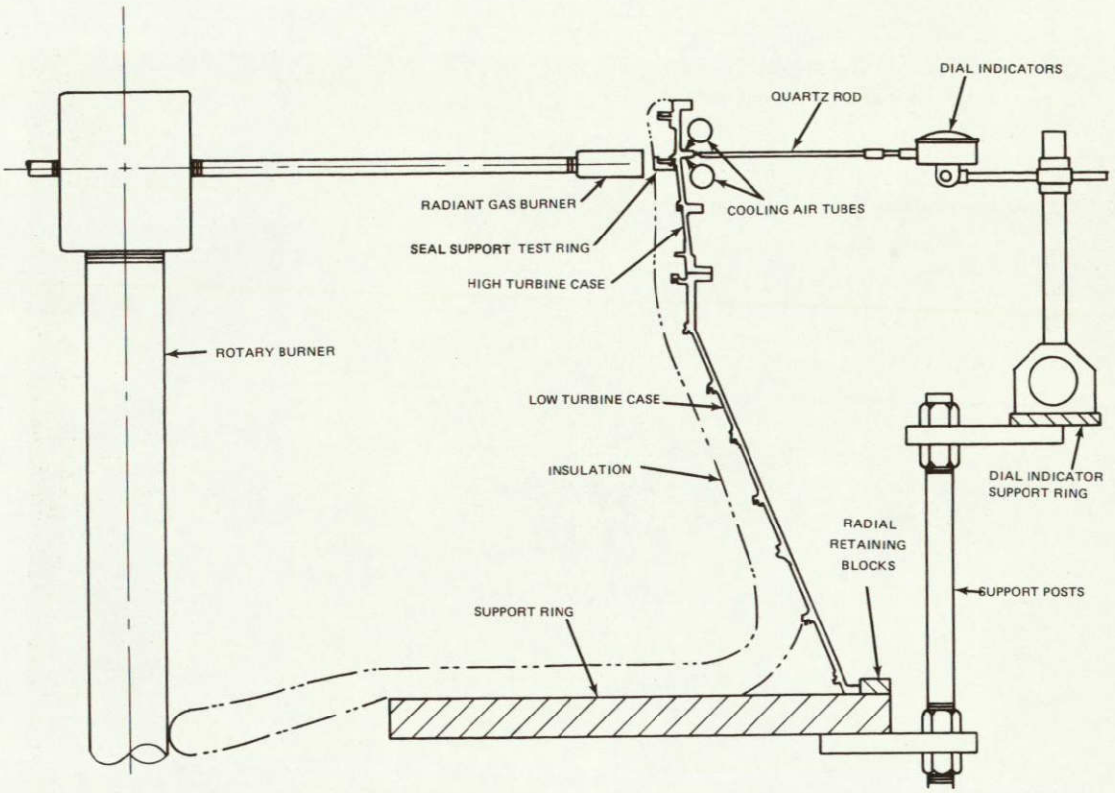

Figure 4-12 Schematic Diagram of Slippage Rig

Dial indicators were mounted at 26 equally spaced locations around the circumference of the case to measure its radial growth. The dial indicators were attached to the rig support ring, which was fixed to ground. Quartz rods were attached to the dial indicators and used as feelers for case radial growth. Quartz was used because it has a low coefficient of expansion, and therefore would not contribute significantly to deflections registering on the dial indicators.

The temperature of the system was measured with 39 thermocouples embedded in the seal support and case. A diagram showing the location of the dial indicators and thermocouples is provided in Figure 4-13.

4.4.2 Test Facility

Testing of the slippage rig was conducted at the Structures Test Laboratory on the Rotary Burner Table facility. The burner table consists of eight radiant gas burners which rotate slowly. The rotating burners simulate the uniform heat input to the seal support assembly in the engine. Figure 4-14 is a photograph of the complete rig mounted in the test stand.

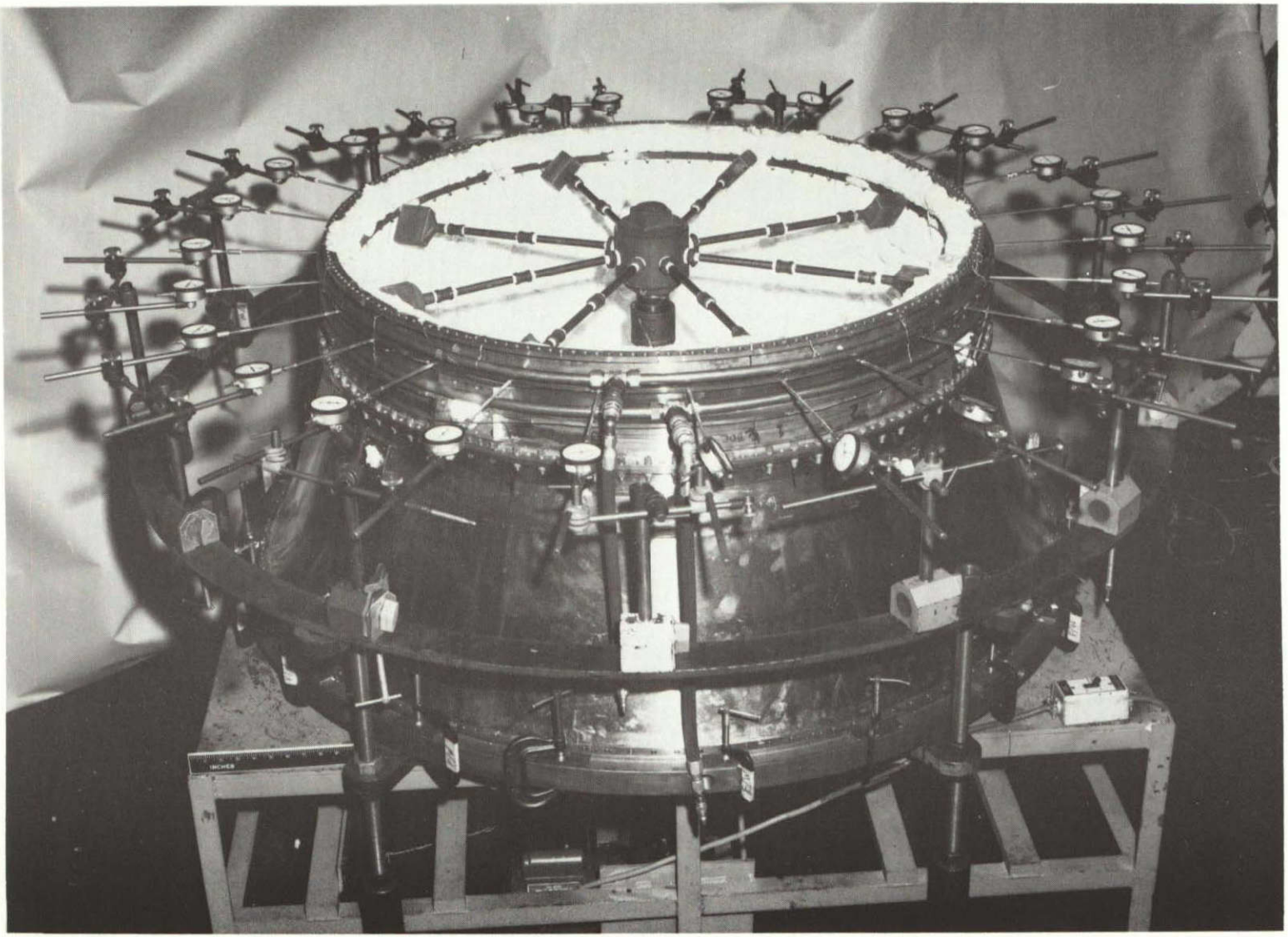

Figure 4-13 Slippage Rig

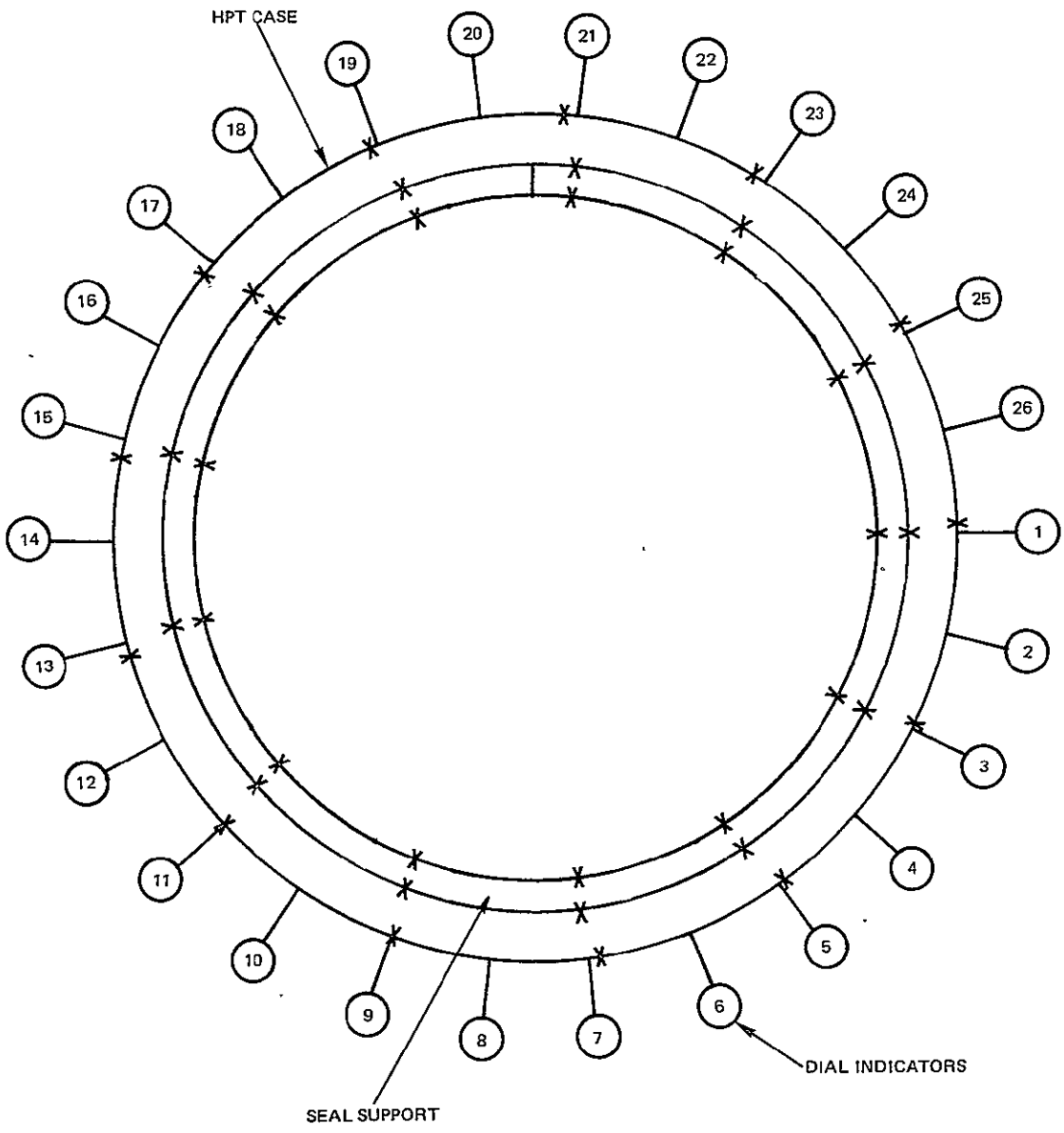

Figure 4-14 Slippage Rig Thermocouple and Dial Indicator Locations

4.4.3 Test Procedure

Three basic test configurations were used: a baseline configuration which simulated the in-service JT9D-7.0/59 high pressure turbine case/outer air seal assembly configuration, and two modifications thereof. Modification I changed the seal support configuration and reduced the number of attaching bolts to one third of the baseline number. Modification II used the Mod I seal support configuration with the baseline bolting arrangement, but with variations in the torque applied to the attaching bolts.

The baseline configuration was tested first. The seal support was mounted in the test rig and the dial indicators were adjusted to zero. The impingement cooling air for the outside of the HPT case was turned on and the inside diameter of the seal support was heated uniformly by the radiant gas burner until a gradient of 472°C (850°F) existed between the inside diameter of the support and the outside diameter of the case flange. This temperature gradient, as determined by engine test, is the maximum value reached by an engine during operation with the ACC system activated. When the system had stabilized at this gradient, dial indicator and temperature measurements were taken. The test was concluded by marking the seal support and case so that they could be assembled in the same relative position for the next series of tests.

The seal support was then removed, modified and reassembled with the turbine case in exactly the same relative position as before, using only 26 attaching bolts (torqued to 9.6 N-m or 85 in-lbs) instead of the original 78 bolts. This test configuration is hereafter referred to as Mod I. The test procedure was then repeated.

At the conclusion of the second test the number of attaching bolts was increased back to 78 with the original 26 still torqued to 9.6 N-m (85 in-lbs) and the additional 52 torqued to 1.8-2.0 N-m (16-18 in-lbs). The test was again repeated. This test configuration is hereafter referred to as Mod II.

The Mod II configuration was then tested again with the torque on the 52 additional bolts reduced to 0.56-1.1 N-m (5-10 in-lbs). This configuration is hereafter referred to as Mod IIA.

5.0 RESULTS

The potential for a TSFC improvement of 0.65 percent over the initial Bill-of-Materials active clearance control configuration was indicated by the simulated altitude engine performance test. The test results from the blowing rig indicate that a small reduction in cooling air is possible in the prototype pipe design, but the improvement is equivalent to no more than 0.03 percent change in TSFC. The Mod I seal support assembly which was evaluated during the engine performance and deterioration testing was the best configuration tested in the slippage rig. Deterioration testing revealed that the improved ACC system did not affect the performance deterioration rate of the engine.

5.1 Simulated Altitude Engine Performance Test

The improved ACC system has the potential for improving cruise TSFC by 1.35 percent compared to an engine without active clearance control. Since the active clearance control system on the initial production JT9D-70/59 engines provides a cruise TSFC improvement of 0.7 percent, the net advantage of the improved ACC system is 0.65 percent. These results are based on data obtained during the simulated altitude performance testing described in Section 4.1.2, extrapolated to compensate for a unique HPT case out-of-round condition in the test engine.

A curve of TSFC improvement obtained in the altitude test at 90 percent maximum cruise thrust is shown in Figure 5-1. The results are plotted versus HPT clearance reduction which was determined analytically based on case temperature data taken in the same test. The base for both the TSFC and clearance scale is the initial run of the engine with the ACC system turned "off". The maximum TSFC improvement demonstrated was 1.05 percent at a closure of 0.56 mm (0.022 in.). However, this result can be extrapolated to a TSFC improvement of 1.35 percent with a further closure of 0.18 mm (0.007 in.), as shown in Figure 5-1. This extrapolation is based on the elimination of a local blade tip rub encountered in the engine test, as described below.

Simulated cruise TSFC data from Figure 5-1 is replotted against HPT case temperature reduction in Figure 5-2. The maximum measured TSFC improvement of 1.05 percent was found at a case temperature reduction of 122°C (220°F). When the case temperature was reduced further, engine performance was degraded. Inspection of the engine parts after the test revealed that the HPT blade tips had been worn away approximately 0.25 mm (0.010 in.) as a result of a rub against a local high spot on the outer air seal shoes. Since this rub was encountered with less case temperature reduction than was anticipated, the roundness of the HPT case, which determines the roundness of the outer air seal, was checked.

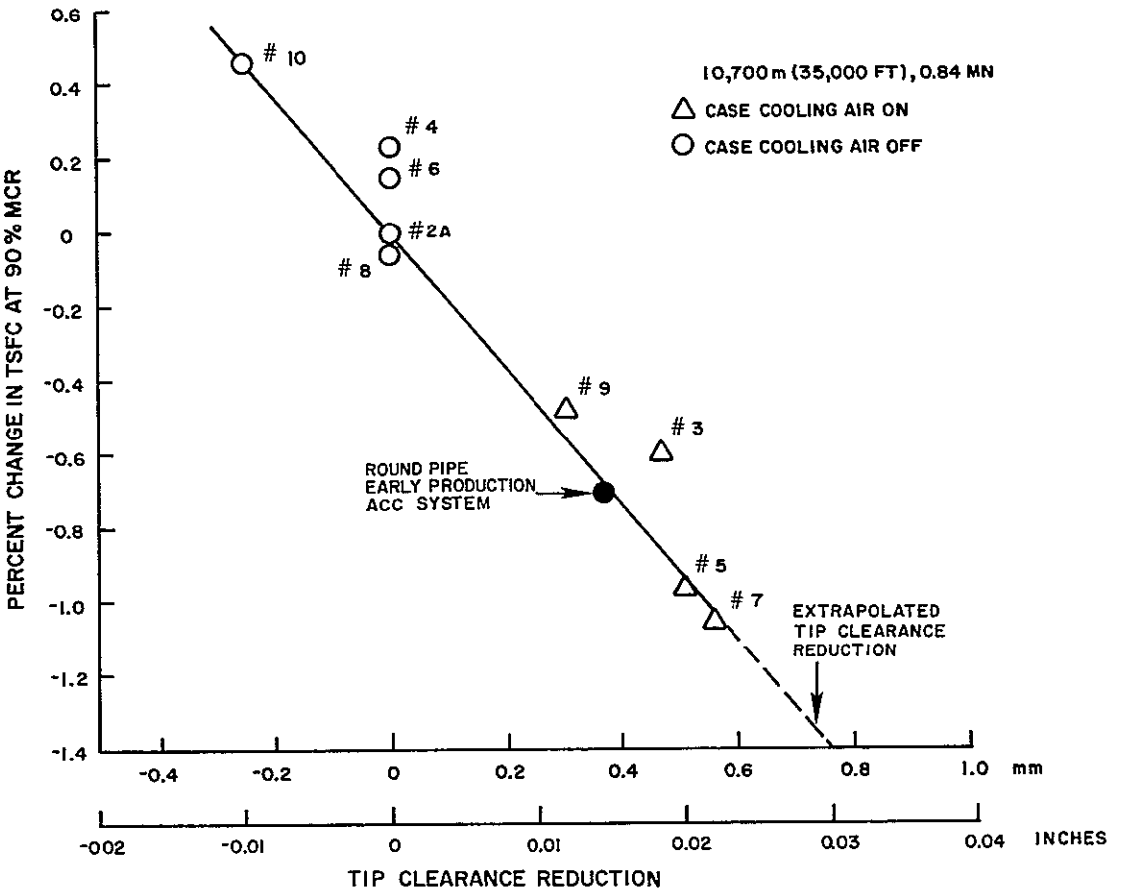

Figure 5-1 *TSFC vs Clearance Reduction at 90 Percent Maximum Cruise Power. See Table 5-1 for identification of run numbers.*

The shape of the HPT case under engine operating conditions can be inferred from the rub depth and pattern on the abradable seal land that is supported between the first and second stage HPT disks by the second stage vanes. A roundness check on the test engine HPT case was made and compared to typical JT9D-70 production engines with extensive airline service. This inspection revealed the case, as installed on the test engine used during this program, was out of round 0.30 mm (0.012 in) more than typical JT9D-70 service cases. This excessive out of roundness was found to be due to the influence of the diffuser case (See Figure 3-1) used on the experimental engine. This case had become badly distorted due to the many repairs and reworks it had undergone during its experimental life. Because of this unrealistic influence, it was considered appropriate to extrapolate the potential TSFC improvement beyond that demonstrated. Rather than take full credit for the 0.30 mm (0.012 in) excessive distortion, the data was conservatively extrapolated only 0.18 mm (0.007 in) additional clearance reduction as shown on Figure 5-1.

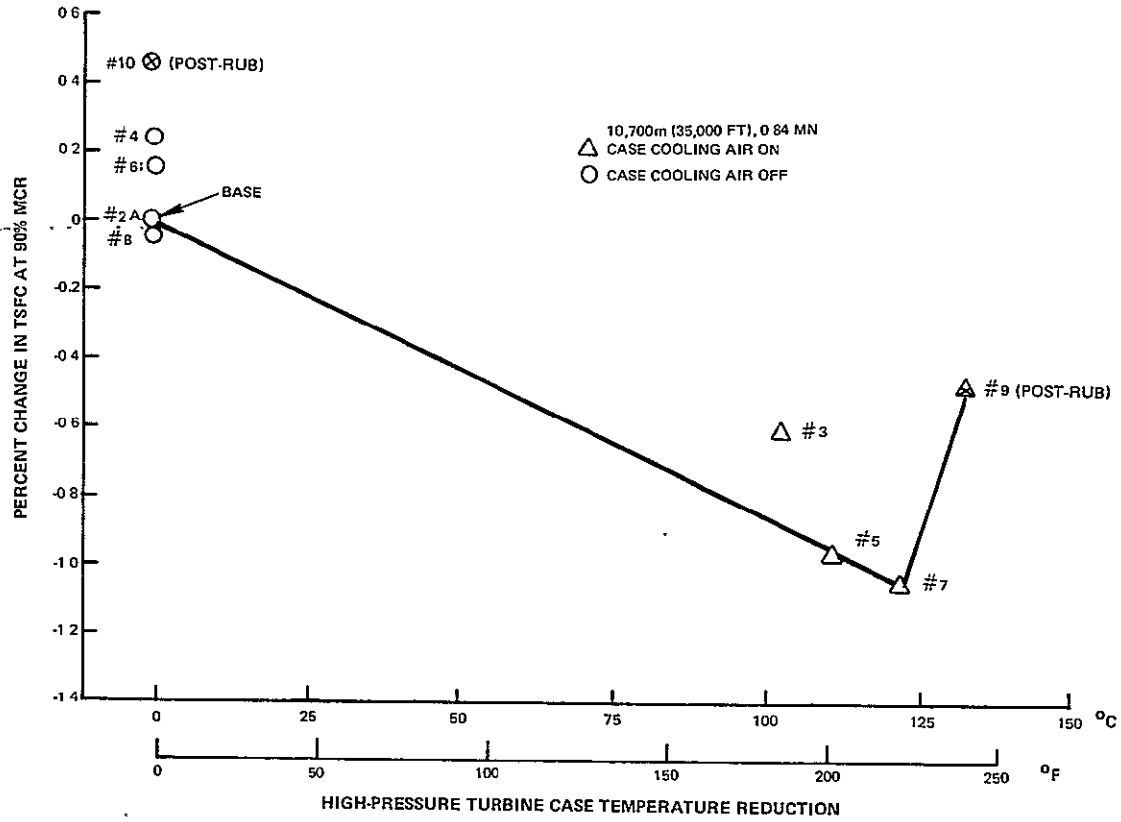

Figure 5-2 TSFC vs HPT Case Temperature Reduction. See Table 5-1 for identification of run numbers.

All of the TSFC data discussed above is based on a 90 percent Max Cruise thrust condition. The potential TSFC improvement in the engine tested relative to the early production engines is plotted against thrust in Figure 5-3 to show that the 90 percent Max Cruise thrust condition is representative of the entire cruise thrust range.

The reduced data from the engine test, covering the complete spectrum of power settings and case temperature reductions, is summarized in Tables 5-1 and 5-2. The TSFC effects and blade tip clearances are presented as differences from the initial test run with the ACC system turned off. The case temperatures represent a weighted average of the thermocouples on the HPT case. The blade tip clearances were calculated based on the average case temperature using a free ring thermal expansion analysis.

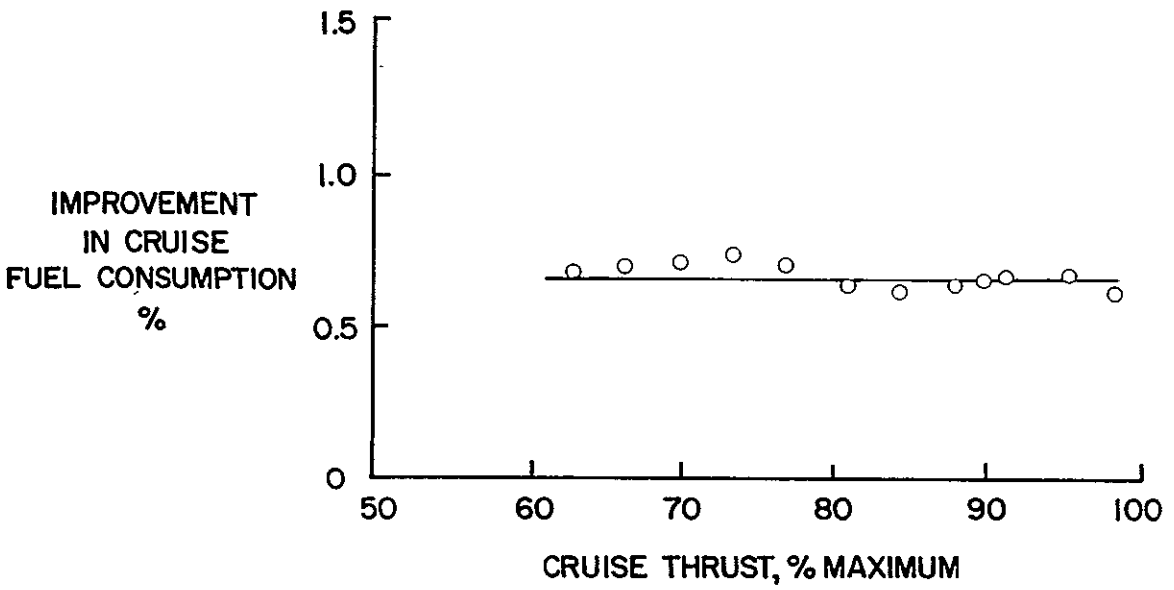

Figure 5-3 Improvement in TSFC Cruise Thrust Relative to Early Production Engines

TABLE 5-1

ENGINE ALTITUDE PERFORMANCE TEST
CASE TEMPERATURE REDUCTION AND CLEARANCE REDUCTION
X-620-12 ENGINE

Calibration #	Cooling Air	Case Temperature Reduction-°C (°F)	Calculated Blade Tip Clearance Reduction mm (in.)
2A	Off	0	Base
3	On	103 (185)	0.47 (0.0185)
4	Off	0	0
5	On	111 (200)	0.51 (0.020)
6	Off	0	0
7	On	122 (220)	0.56 (0.022)
8	Off	0	0
9	On	133 (240)	0.30 (0.012)
10	Off	0	0.25 (0.010) incr.

TABLE 5-2

ENGINE ALTITUDE PERFORMANCE TEST
TSFC REDUCTION
X-620-12 ENGINE

% MCR Thrust	Calibration # 2A	3	4	5	6	7	8	9	10
				% TSFC Change					
62.8	Base	-0.87	-0.25	-0.98	-0.38	-1.08	0.0	-0.89	0.50
66.4	Base	-0.71	-0.10	-0.93	-0.16	-1.10	-0.10	-0.74	0.49
70.0	Base	-0.61	-0.01	-0.90	-0.03	-1.14	-0.20	-0.60	0.35
73.6	Base	-0.57	0.06	-0.94	0.04	-1.17	-0.25	-0.53	0.26
77.1	Base	-0.54	0.06	-0.94	0.04	-1.12	-0.24	-0.47	0.31
80.8	Base	-0.55	0.16	-0.91	0.15	-1.02	-0.16	-0.44	0.37
84.4	Base	-0.56	0.18	-0.93	0.13	-0.99	-0.06	-0.43	0.43
88.0	Base	-0.60	0.24	-0.94	0.13	-1.02	-0.06	-0.47	0.44
91.6	Base	-0.57	0.27	-0.96	0.15	-1.06	-0.06	-0.46	0.44
95.2	Base	-0.57	---	-0.96	---	-1.06	---	-0.38	0.49
98.7	Base	-0.50	---	-0.92	000	-0.97	---	-0.15	0.51

5.2 Engine Performance Deterioration Test

Performance calibrations run on a JT9D-70/59 engine with an improved ACC system at sea level conditions after the 1000 cyclic endurance test indicated—that the engine performance deteriorated (TSFC increased) relative to the performance run prior to the cyclic endurance tests. The deterioration in performance was slightly less than the average deterioration experienced on a number of other engines with early production ACC systems run through similar cyclic endurance tests. These limited test results indicate that the improved ACC system apparently does not affect engine performance deterioration characteristics.

The reduction in TSFC from actuating the improved ACC system at a number of thrust levels is shown in Table 5-3 for performance calibrations run before and after the cyclic endurance test. The average pre-cyclic TSFC reduction of 2.36 percent and post-cyclic TSFC reduction of 1.95 percent is equivalent to about 1.2 and 1.0 percent TSFC reduction respectively at the 10,700 m (35,000 ft), 0.84 Mach number cruise operating condition run during the altitude performance tests. This indicated 20 percent reduction in effectiveness of the active clearance control system is not substantiated by post test parts inspection. It is suspected that since the cooling air to the ACC was supplied by the test stand compressed air system instead of bleeding the fan, the airflow rate to the ACC system was inadvertantly reduced for the post-endurance calibrations, but no cooling airflow data or HPT case temperatures were recorded during the test to prove these suspicions.

TABLE 5-3

ENGINE DETERIORATION TEST
TSFC REDUCTION
ENGINE X-622-12

Corrected Thrust -Newtons (lbf)		Pre-Cyclic % Change in TSFC	Post-Cyclic % Change in TSFC
80,000	(18,000)	-2.46	
89,000	(20,000)	-2.46	-2.04
98,000	(22,000)	-2.46	-2.04
107,000	(24,000)	-2.46	-2.04
110,000	(26,000)	-2.40	-1.95
125,000	(28,000)	-2.31	-1.89
133,000	(30,000)	-2.19	-1.86
142,000	(32,000)	-2.12	-1.85
Average		-2.36	-1.95

5.3 Blowing Rig Test

The blowing rig test results indicate that a small reduction in cooling airflow can be achieved by increasing the spacing in two of the five rows of holes in the simulated prototype pipe. If similar reductions were possible in all of the engine cooling pipes of the ACC systems, the result would be a 9 percent reduction in fan bleed air requirements, which is equivalent to a TSFC improvement of about 0.03 percent. These modifications were not incorporated in the final design because the additional test time and expense did not appear justified by the small fuel savings.

Data from the rig tests was reduced to heat transfer coefficients and cooling airflow rates for the bolted and non-bolted flanges independently. The results at the minimum and maximum tested values of impingement pressure ratio, respectively, are plotted on Figures 5-4 and 5-5 for the bolted side, and 5-6 and 5-7 for the non-bolted side. Both sets of plots are based on the 1500 watt input power case. The other power levels gave similar results, as indicated by the 1000 watt input power points plotted on Figures 5-5 and 5-7.

The results for the bolted side of the system (Figures 5-4 and 5-5) show that none of the tested configurations equalled the heat transfer coefficient of the prototype configuration (configuration 1) with less airflow. However, the results on the non-bolted side (Figures 5-6 and 5-7) show that configuration 11 approximately equals the heat transfer coefficient of the prototype configuration with 18 percent less airflow. Combining the non-bolted side of configuration 11 with the bolted side of configuration 1 would result in an airflow reduction of 9 percent in the cooling pipe simulated in the test rig.

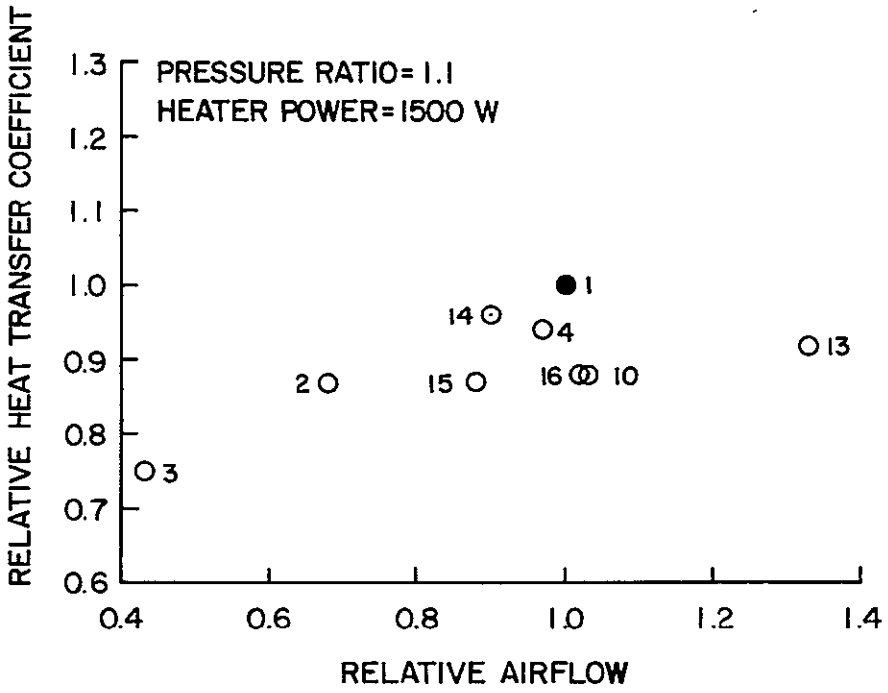

Figure 5-4 *Relative Heat Transfer Coefficient Versus Relative Cooling Airflow Results for Bolted Flange. See Table 4-3 for identification of run numbers.*

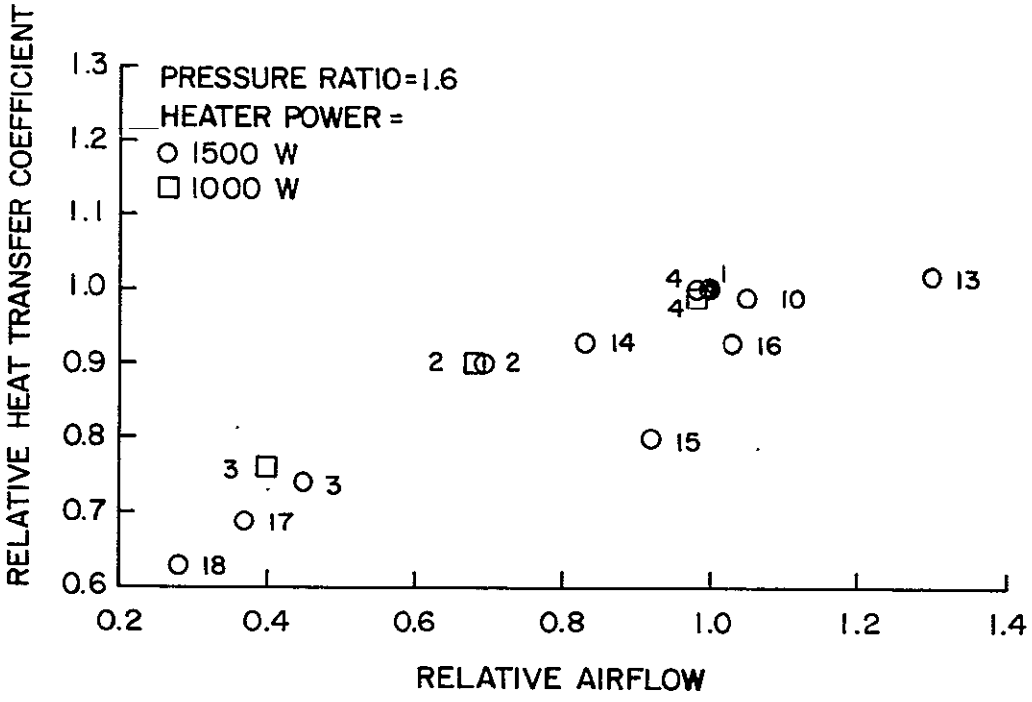

Figure 5-5 *Relative Heat Transfer Coefficient Versus Relative Cooling Airflow Results for Bolted Flange. See Table 4-3 for identification of run numbers.*

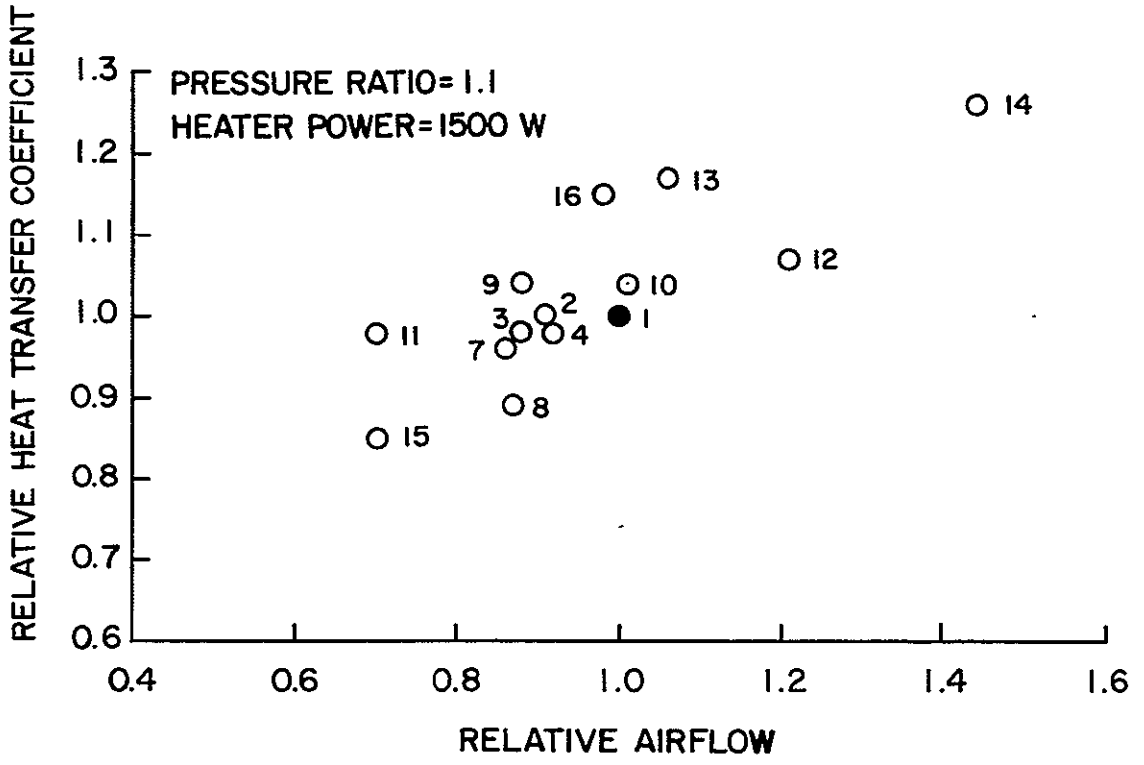

Figure 5-6 *Relative Heat Transfer Coefficient Versus Relative Cooling Airflow Results for Non-Bolted Flange. See Table 4-3 for identification of run numbers.*

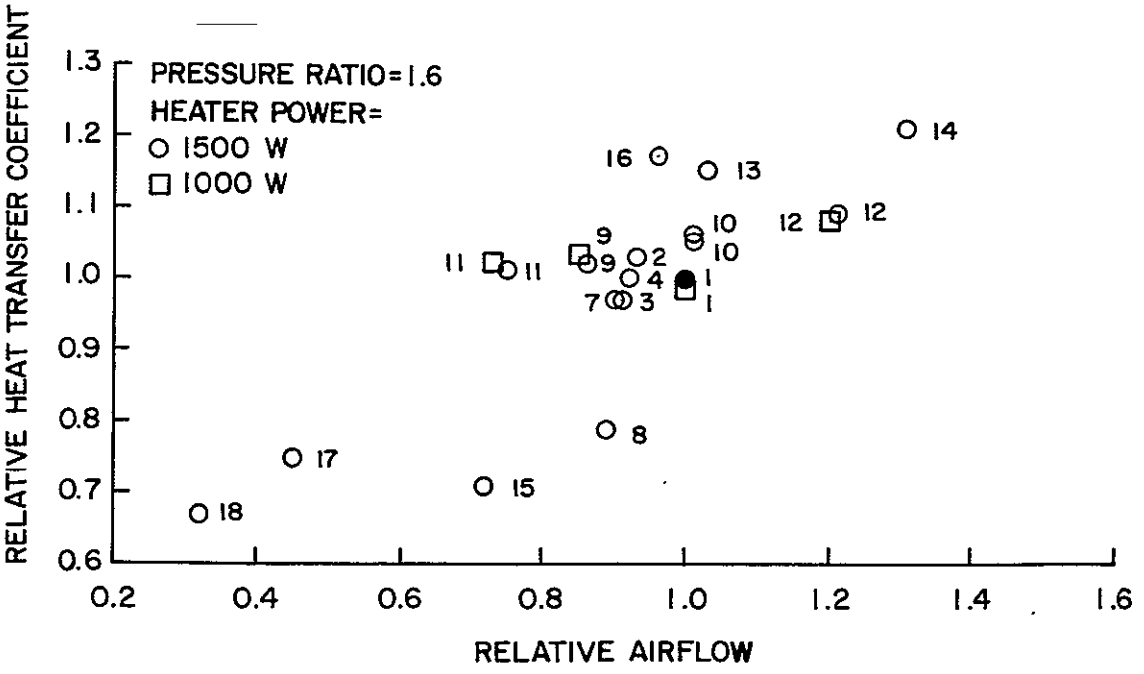

Figure 5-7 *Relative Heat Transfer Coefficient Versus Relative Cooling Airflow Results for Non-Bolted Flange. See Table 4-3 for identification of run numbers.*

The figures also show that the choice of cooling configuration is not affected significantly by the impingement ratio over the range tested. The lower end of the range (1.1 pressure ratio) provides a Reynold's number equal to that of the engine system operating at typical cruise conditions. The upper end of the range (1.6 pressure ratio) represents the upper limit that might be achievable on an engine system at cruise conditions with the engine operating at high power and with a very low pressure drop supply system. Consequently, the results for this condition indicate the maximum cooling capabilities of the configurations tested.

The heat transfer coefficients for Figures 5-4, 5-5, 5-6 and 5-7 were integrated over the area covered by the thermocouples on each side of the rig, using the following equation:

$$h = \frac{Q}{\sum_{1}^{n} (T_i - T_{air})\, A_i}$$

where: h = heat transfer coefficient
T = flange temperature
T_{air} = cooling air temperature
A = incremental flange area
Q = power input
n = number of area increments
i = flange increment number

The basic rig test results are plotted in the form of the difference between average flange temperature and air temperature versus airflow in Figures 5-8 through 5-14. The ordinate of these figures is inversely proportional to heat transfer coefficient, so lower temperature differences imply a higher effectiveness of the cooling system. The symbols represent actual data points, with the highest flow for any configuration always being at an impingement pressure ratio of 1.6. Adjacent points represent a pressure ratio difference of 0.1. The lowest flow represents a pressure ratio of 1.1 for the 6 point curves and 1.2 for the 5 point curves.

Figure 5-8 shows the effect of varying hole diameter in the first two rows of cooling holes. These are the holes that cool the bolted flange. Comparing configurations 4, 2 and 3, in that order, shows a trend toward lower ccoling airflow for a given temperature difference, but with the requirement for increasing impingement pressure ratio. This requirement implies a reduction in the maximum cooling capacity with the smaller holes. The prototype configuration (1) does not fit the trend exactly because its number of holes in rows 1 and 2 is different from the others, but it is included for comparative purposes.

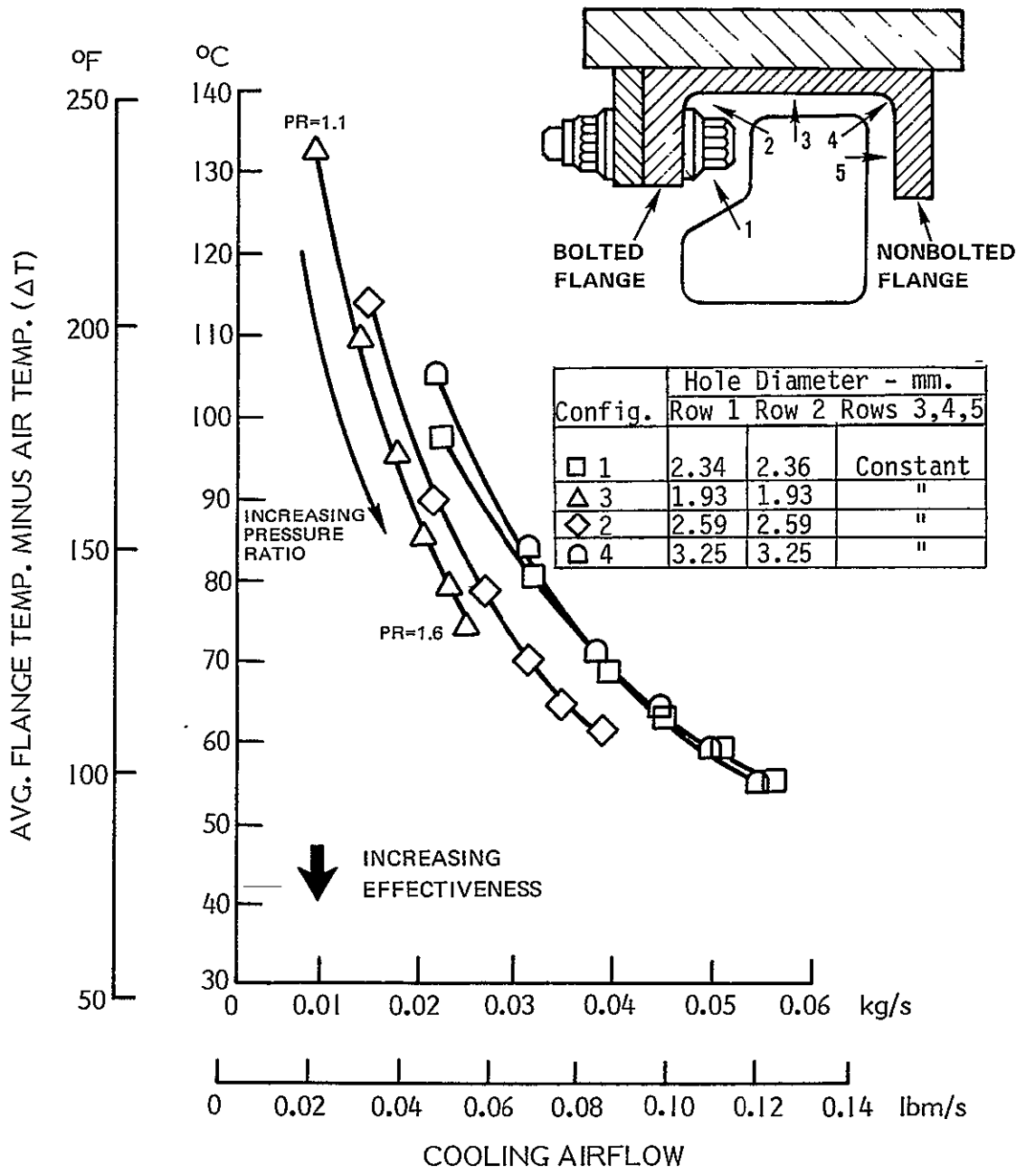

Figure 5-8 *Effect of Varying Hole Diameter on the Heat Transfer Effectiveness for the Bolted Side. The impingement pressure ratio varies as shown for all remaining figures. Heater power is set at 1500 watts.*

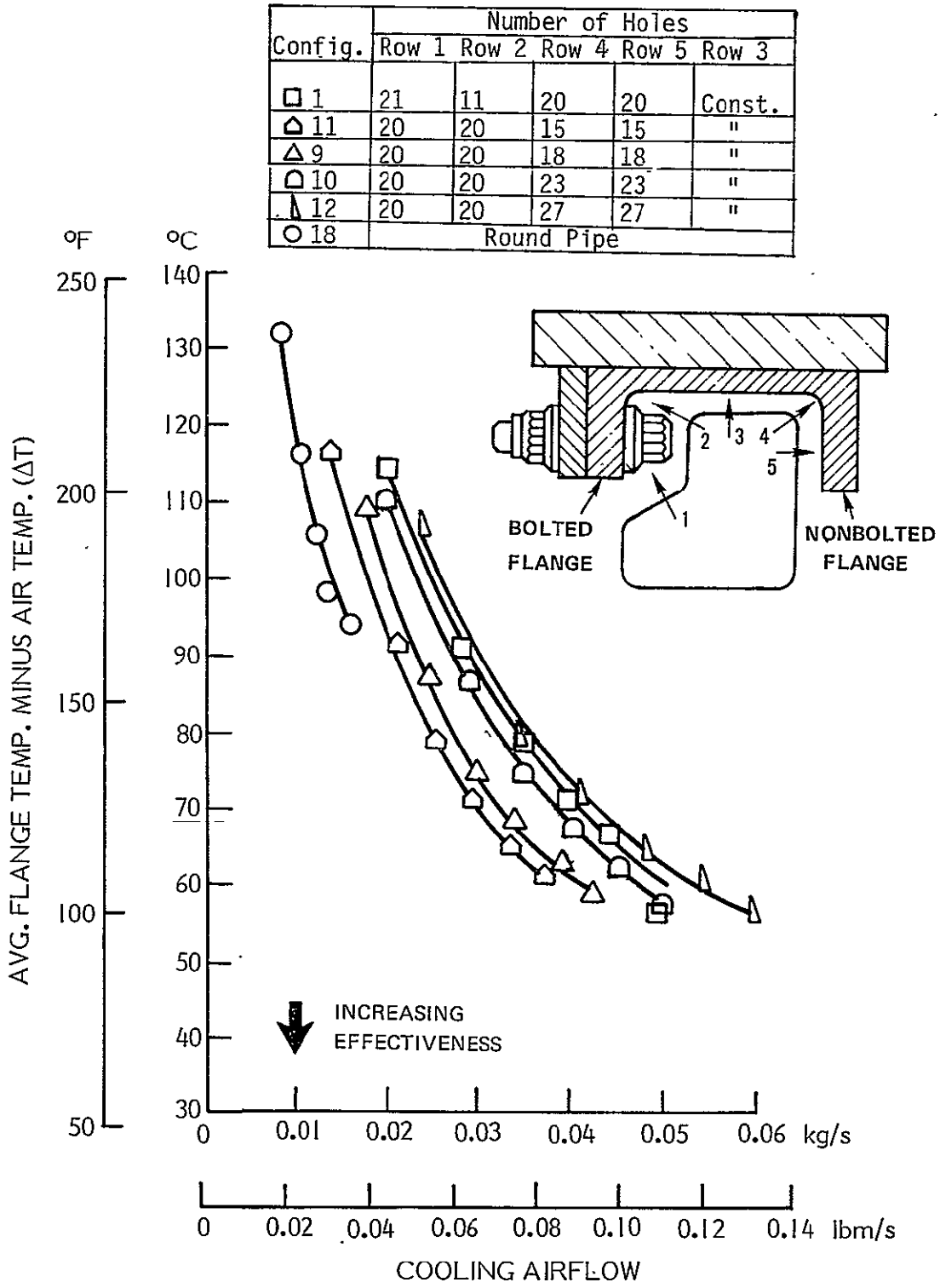

Figure 5-9 *Effect of Varying the Number of Holes on the Heat Transfer Effectiveness for the Non-Bolted Side. Heater power is set at 1500 watts.*

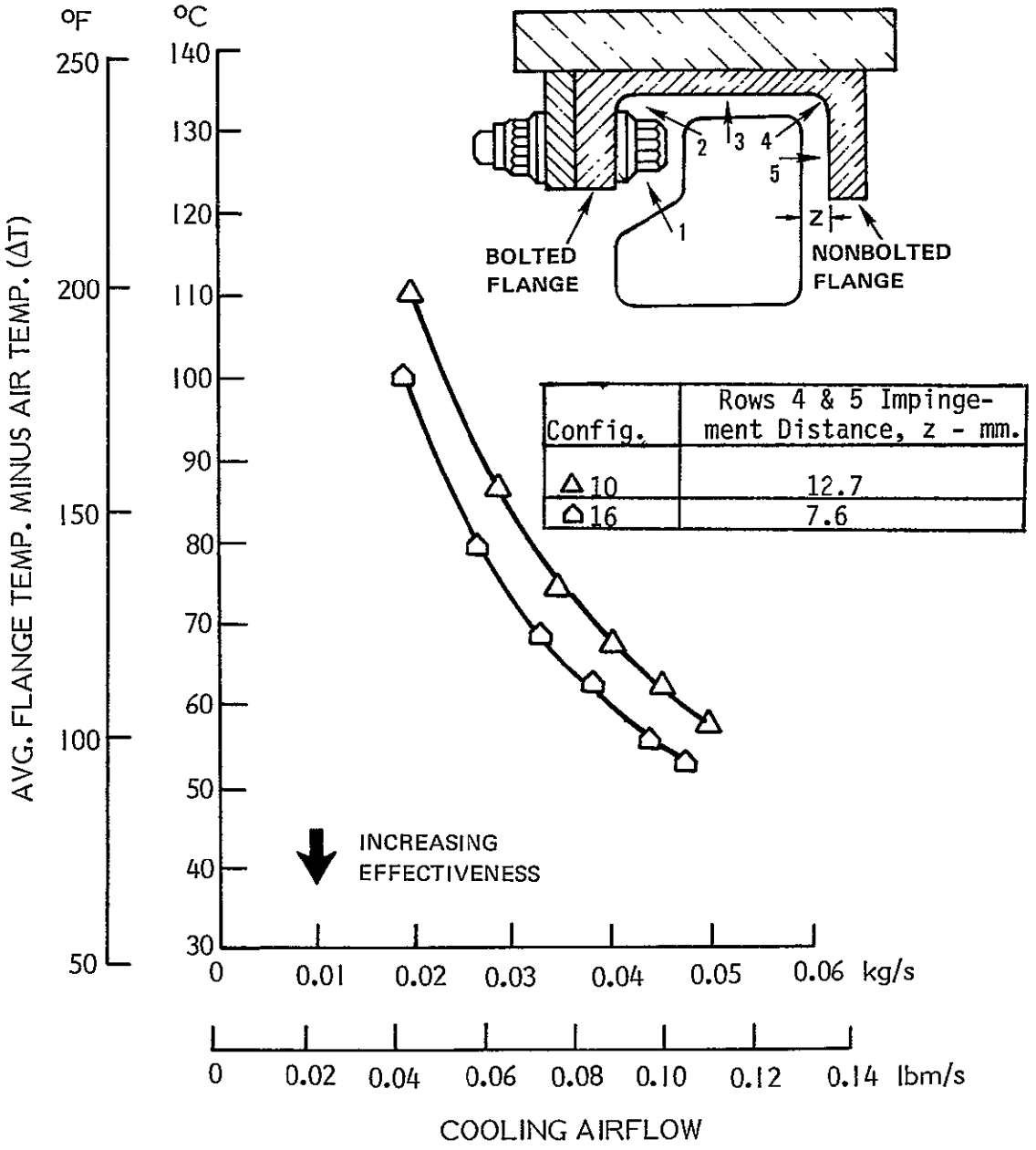

Figure 5-10 *Effect of Varying Impingement Distance on the Heat Transfer Effectiveness for the Non-Bolted Side. Heater power is set at 1500 watts.*

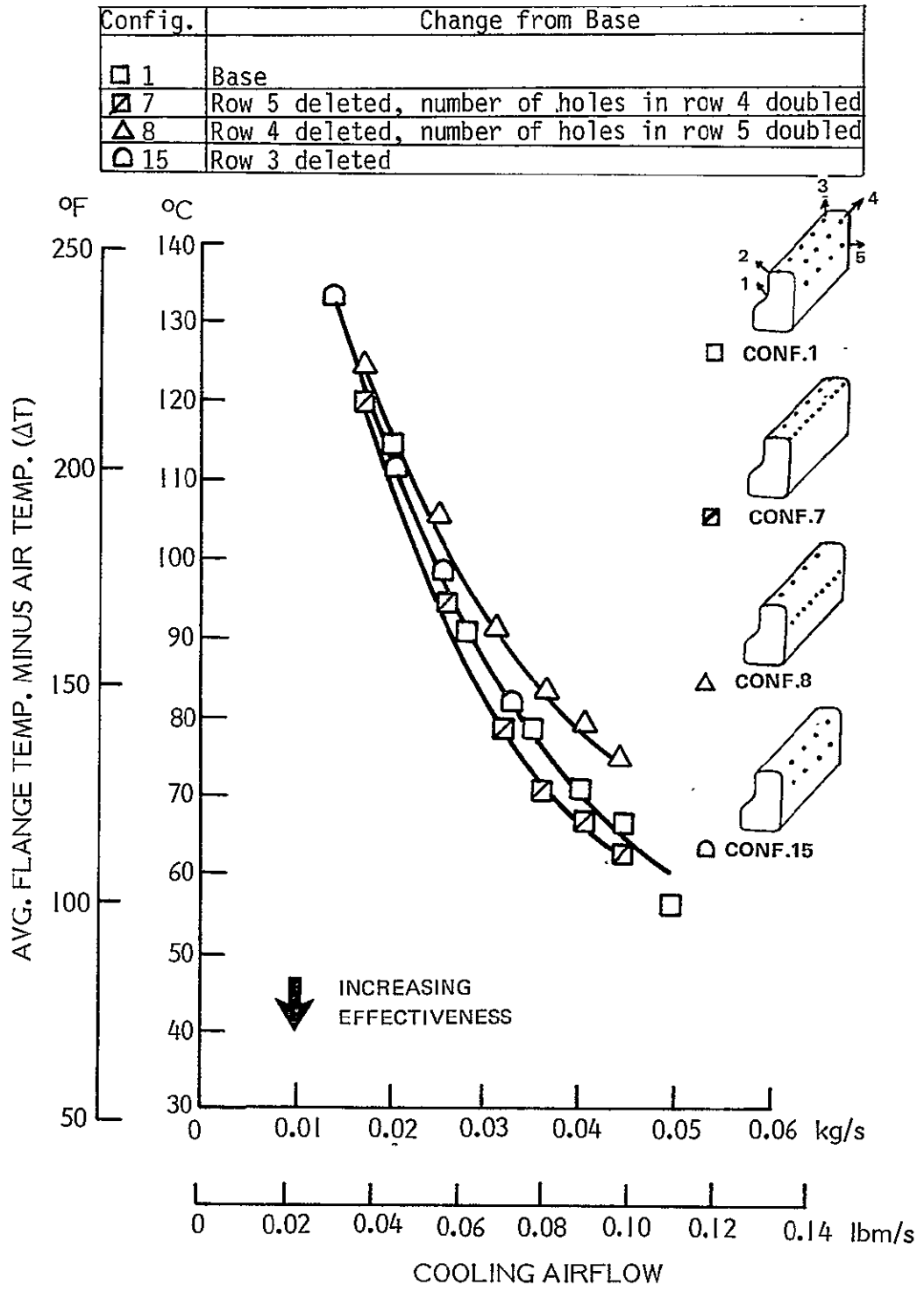

Figure 5-11 Effect of Hole Location on the Heat Transfer Effectiveness for the Non-Bolted Side. Heater power is set at 1500 watts.

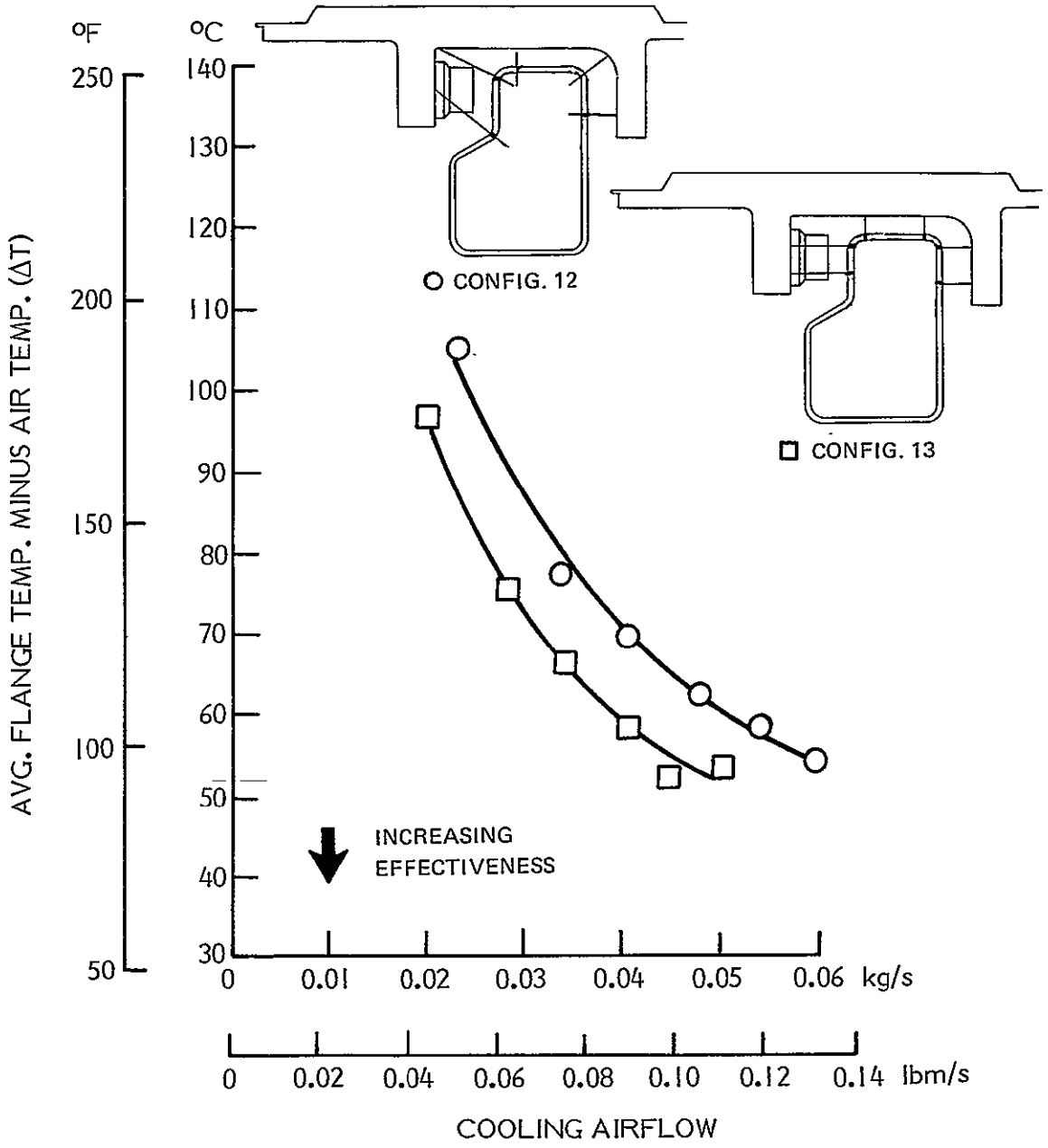

Figure 5-12 *Effect of Varying Impingement Angle on the Heat Transfer Effectiveness for the Non-Bolted Side. Configuration 12 uses an angular impingement scheme, while configuration 13 uses a perpendicular one. Heater power is set at 1500 watts.*

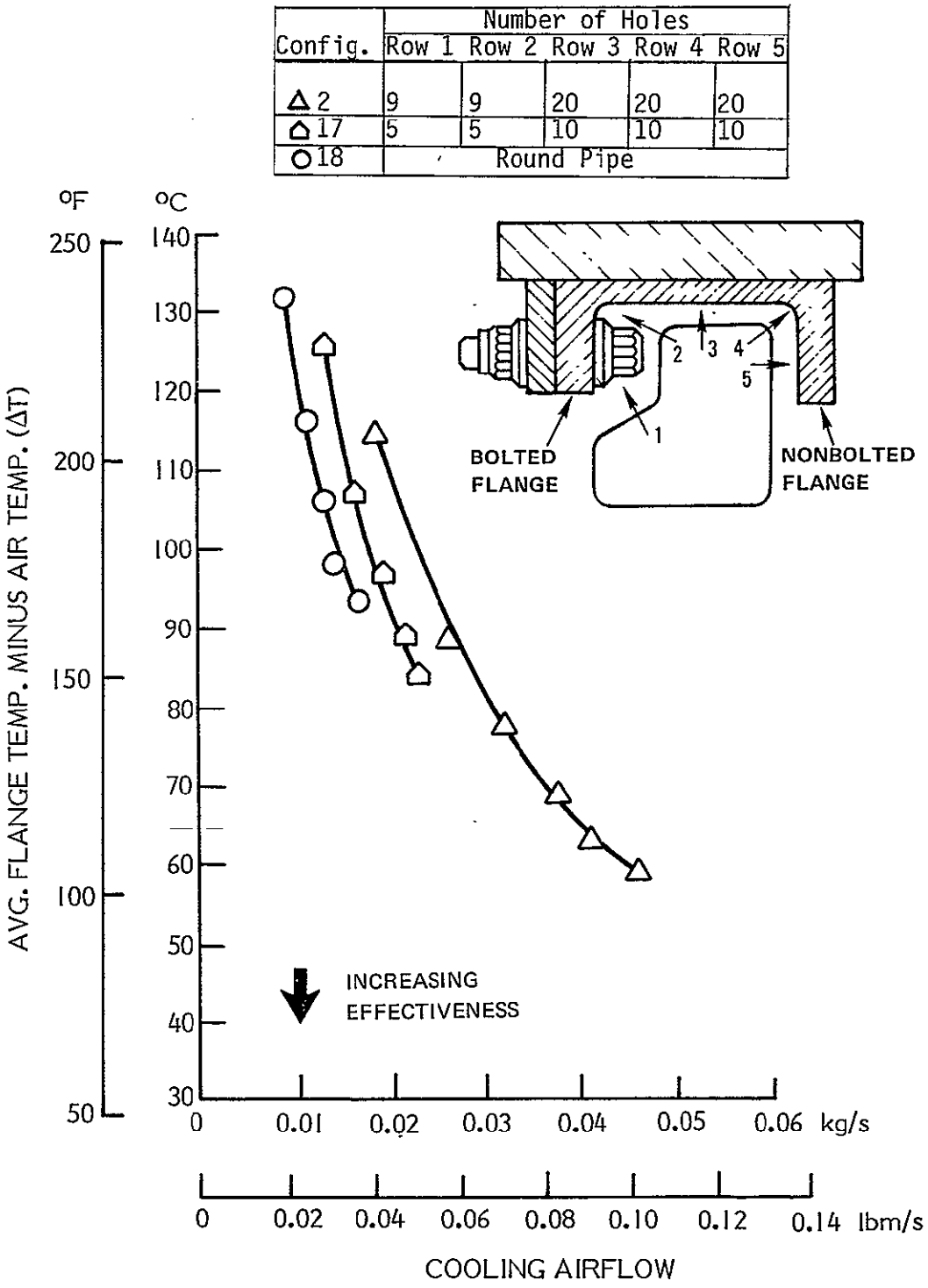

Figure 5-13 Effect of Varying the Number of Holes on the Heat Transfer Effectiveness for the Non-Bolted Side. Heater power is set at 1500 watts.

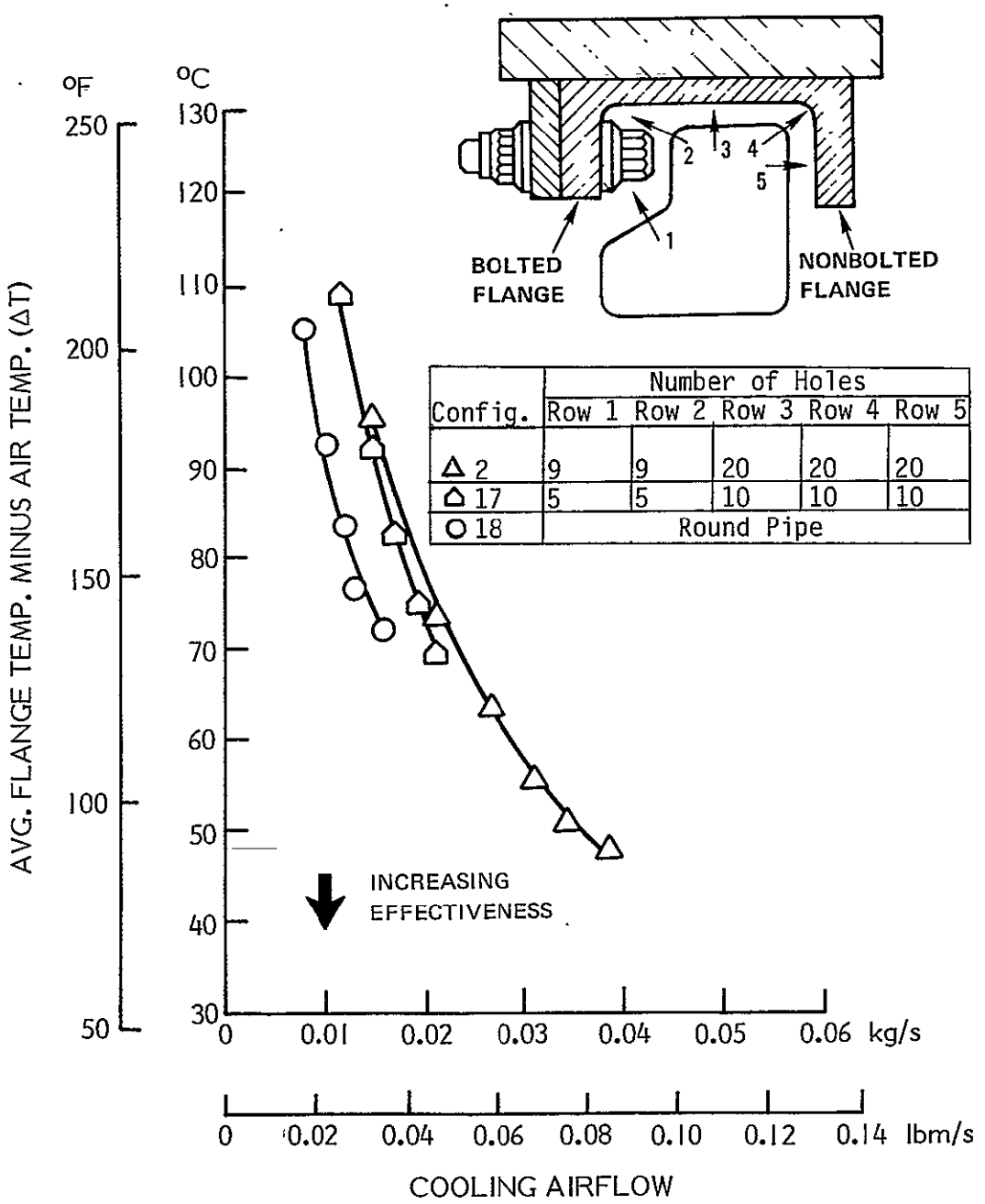

Figure 5-14 *Effect of Varying the Number of Holes on the Heat Transfer Effectiveness for the Bolted Side. Heater power is set at 1500 watts.*

The effect of varying the spacing between the number of holes on the non-bolted side is shown in Figure 5-9. These results indicate that using fewer holes of the same diameter can reduce the cooling flow required for a given temperature difference. The trend can best be seen by comparing configurations 12, 10, 9 and 11, in that order. The prototype configuration (1) does not fit the trend exactly because the number of holes in row 2 is inconsistent with the others, but it is shown for comparative purposes. Configuration 18, round cooling pipes simulating the configuration used on early production engines, is also shown only for comparative purposes.

The effect of reducing the impingement striking distance is shown in Figure 5-10. The impingement distance to the nonbolted flange of the baseline configuration was reduced from 1.27 to 0.76 cm (0.50 to 0.30 in.). These test results indicate that decreasing this distance improves the cooling effectiveness of the system by about 10 percent.

Figure 5-11 shows the effect of redistributing the rows of impingement holes in the pipe. These test results indicate that the cooling effectiveness is greatest when the cooling air is directed at the base of the flange and at the HPT case. This is because these locations are at a higher temperature, and the air remains in the cavity for a longer period of time, enabling it to absorb more heat. Configuration 1 (the prototype) distributes the flow evenly between the base and O.D. of the flange. Configuration 7 eliminates the row of cooling holes (row 5) directed at the O.D. of the non-bolted flange, but maintains total flow by increasing the number of holes directing cooling air at the I.D. (base) of the flange. Configuration 8 directs the flow at the O.D. of the flange but not at the base. Configuration 15 has the same hole pattern directing flow at the flanges as configuration 1 but it eliminates the middle row (row 3) of holes which direct cooling air at the case. For a given flow, this configuration has the same cooling effectiveness as 1, but with a reduced flow capacity.

The effect of changing the air jet impingement angle is shown in Figure 5-12. The test results indicate that a 90° striking angle improves the cooling effectiveness an average of 6 percent. The two configurations are illustrated in the inset. The baseline case (configuration 12) has five rows of airjets, three of which strike the case at an angle. Configuration 13 replaces one of these three rows with two rows having the same total flow area, and relocates the other two rows, so all of its air jets strike perpendicular to the case surfaces.

Figures 5-13 and 5-14 show the effect of reducing the number of holes in all rows by one-half, while retaining the same hole diameter. The effect on the non-bolted side (Figure 5-13) is a significantly lower airflow for a given temperature difference, but with the requirement of increasing impingement pressure ratio (reduction in maximum cooling capacity). The effect on the bolted side (Figure 5-14) is to reduce maximum cooling capacity without a significant improvement in effectiveness. Configuration 18 is shown only for comparative purposes.

5.4 Slippage Rig Test

The test results of the various seal support configurations run in the slippage rig indicate that the Mod I seal support produces the minimum and most uniform radial expansion of the HPT case. Mod I is the configuration evaluated during the engine test described in Sections 5.1 and 5.2.

A tabulation of the average radial growth and the maximum deviation from the average is presented in Table 5-4 for each of the test configurations.The tabulation shows that the three modified configurations have approximately the same average radial growth. This growth is about 40 percent less than the baseline case, which represents the early production seal support configuration. The reduced average radial growth implies that substantially less cooling airflow is needed with the modified configurations to accomplish the desired reduction in turbine tip clearance.

TABLE 5-4

SLIPPAGE RIG TEST
RADIAL GROWTH

Test Configuration	Average Radial Growth and Max. Deviation	
	mm	inches
Baseline	2.41 + 0.43 - 0.48	0.095 + 0.017 - 0.019
Mod I	1.46 + 0.15 - 0.20	0.058 + 0.006 - 0.008
Mod II	1.55 + 0.46 - 0.79	0.062 + 0.018 - 0.031
Mod IIA	1.58 + 0.41 - 0.43	0.061 + 0.016 - 0.017

Table 5-4 also shows that Mod I has significantly less deviation from the average radial growth than the other three configurations, which implies that it will result in relatively less out-of-roundness of the turbine tip seals in the engine. The absolute out-of-roundness of the engine seal cannot be inferred from this data, since the rig did not simulate the pressure and bending loads encounterd by an operating engine.

5.5 Economic Evaluation

The improved ACC concept was evaluated as part of the ECI-PI Task 1 Feasibility Analysis effort (Ref. 1) in 1977 to estimate its acceptability to the airline companies and the cumulative fuel saving that would result if it became part of the engine Bill-of-Materials. This

evaluation was based on analytical estimates of the effects of the concept on engine performance, weight, and cost. These original engine and airplane performance estimates are shown in the first column of Tables 5-5, 5-6 and 5-7. It was on the basis of this original evaluation that the improved ACC concept was chosen for demonstration under the ECI-PI program. The second column of the tables shows the performance improvement that resulted from the engine test program to be smaller than the estimate made in 1977. Note that the earlier estimates of engine weight and price effects, and the projected start of service date have not been updated, since the engine test program provided no new information on these parameters.

TABLE 5-5

JT9D-70/59 HPT IMPROVED ACC
PREDICTED EFFECTS ON ENGINE (Per Engine)

	Original Evaluation	Revisions Based On Test Results
TSFC Improvement, %	-	
Takeoff	-	
Climb		
Cruise, avg.	0.9	0.65
Hold	-	
EGT Improvement, °C		
Takeoff	-	
Climb	-	
Weight Change, Kg(lb)	+34(+75)	
Price Change, $	+13,400	
Kit Price, $ (non-attrition basis)	80,600	
Maintenance Cost Change, $/Oper. Hr.		
Materials	0	
Labor @$30 per Man-Hr.	0	
Start of Service Date	Mid 1979	

TABLE 5-6

JT9D-70/59 IMPROVED HPT ACC
AIRLINE COST EVALUATION (Per Airplane)

	Original Evaluation	Revisions Based On Test Results
747-200 Airplane		
Total Operating Cost Change, $/yr.	-76,060	- 55,470
Required Airline Investment Change, $		
New Buy	+ 76,100	
Retrofit	+454,300	
Payback Period, Years		
New Buy	1.0	1.4
Retrofit	6.0	8.2
DC 10-40 Airplane		
Total Operating Cost Change, $/yr.	-28,300	- 20,770
Required Airline Investment Change, $		
New Buy	+ 59,500	
Retrofit	+330,750	
Payback Period, Years		
New Buy	2.1	2.9
Retrofit	11.7	15.9

TABLE 5-7

JT9D-70/59 IMPROVED HPT ACC
FUEL SAVING EVALUATION
WORLD FLEET OF 747 and DC10-40 AIRPLANES

	Original Evaluation	Revisions Based On Test Results
No. of Engines Affected		
New Buy	1150	1150
Retrofit	0	0
Total	1150	1150
Cumulative Fuel Saved, 10^6 Liters (10^6 gal)		
New Buy	1771 (468)	1279 (338)
Retrofit	0	0
Total	1771 (468)	1279 (338)
Fleet Fuel Saved, %	0.9	0.65

The results of the economic evaluation are corrected in the second column of Tables 5-6 and 5-7 to reflect the demonstrated performance improvement. Table 5-6 shows that the payback periods on both airplane models are increased, but the new buy payback periods are still well within the limiting value of 6 years established in the Task I Feasibility Analysis (ref. 1). Consequently, the number of engines affected is unchanged, as shown by Table 5-7. The percent fleet fuel saving estimate has been revised downward to reflect the demonstrated performance of the concept, and the revised cumulative fuel saving has been proportionally reduced to 1279 million liters (338 million gallons).

6.0 CONCLUDING REMARKS

Engine testing of the JT9D-70/59 Improved HPT Active Clearance Control concept shows an average cruise TSFC improvement potential of 0.65 percent more than that offered by the JT9D-70/59 system in service.

The modified system showed no unusual wear or deterioration effects in a 1000 cycle engine endurance test.

The demonstrated TSFC improvement is smaller than the estimate used in the ECI Feasibility Analysis evaluation of the concept. As a result, the estimated payback period has increased, but the new buy value is still well within the acceptable limit. The cumulative fuel saving for the concept (as defined by the Feasibility Analysis) is now estimated at 1279 million liters (338 million gallons).

APPENDIX A

PRODUCT ASSURANCE

INTRODUCTION

The Product Assurance system provided for the establishment of quality requirements and determination of compliance with these requirements, from procurement of raw material until the completion of the experimental test. The system ensures the detection of nonconformances, their proper disposition, and effective corrective action.

Materials, parts, and assemblies were controlled and inspected to the requirements of the JT9D-70/59 Improved High Pressure Turbine Active Clearance Control System Program. A full production-type program requires inspection to the requirements indicated on the drawings and pertinent specifications. On experimental programs Engineering may delete or waive noncritical inspection requirements that are normally performed by Experimental Quality Assurance.

Parts, assemblies, components and end-item articles were inspected and tested prior to delivery to ensure compliance to all established requirements and specifications.

The results of the required inspections and tests were documented as evidence of quality. Such documents, when requested, will be made available to designated Government Representatives for on-site review.

Standard P&WA Commercial Products Division Quality Assurance Standards currently in effect and consistent with Contractual Quality Assurance Requirements were followed during execution of this task. Specific standards were applied under the contract in the following areas:

1. Purchased Parts and Experimental Machine Shop
2. Experimental Assembly
3. Experimental Test
4. Instrumentation and Equipment
5. Data
6. Records
7. Reliability, Maintainability and Safety

1. PURCHASED PARTS AND EXPERIMENTAL MACHINE SHOP

Pratt & Whitney Aircraft has the responsibility for the quality of supplier and supplier-subcontractor articles, and effected its responsibility by requiring either control at source by P&WA Vendor Quality Control or inspection after receipt at P&WA. Records of inspections and tests performed at source were maintained by the supplier as specified in P&WA Purchase Order requirements.

Quality Assurance made certain that required inspections and tests of purchased materials and parts were completed either at the supplier's plant or upon receipt at P&WA.

Receiving inspection included a check for damage in transit, identification of parts against shipping and receiving documents, drawing and specification requirements, and a check for Materials Control Laboratory release. Positive identification and control of parts was maintained pending final inspection and test results.

The parts manufactured in Pratt & Whitney Aircraft Experimental Machine Shop were subject to Experimental Construction procedures to ensure that proper methods and responsibilities for the control of various quality standards were followed.

Drawing control was maintained through an engineering drawing control system. Parts were identified with the foregoing system. Quality Assurance personnel are responsible for reviewing drawings to ensure that the proper inspection requirements are indicated.

Non-conforming experimental articles involved in this program were detected and identified by Experimental Construction, by vendors, or by Experimental Quality Assurance. Non-conforming articles were reviewed by Engineering and Experimental Quality Assurance personnel in deciding disposition. Records of these decisions, including descriptions of the non-conformances were maintained by Experimental Quality Assurance and reviewed by the cognizant Government Quality Assurance Representative.

2. EXPERIMENTAL-ASSEMBLY

In Experimental Assembly two engines were assembled for evaluation of engine performance under the program. Established Experimental Construction procedures were employed to perform the work and to ensure that proper responsibilities and methods for the control of various quality standards were followed.

Two test rigs were assembled in Experimental Assembly for evaluation of variations to the active clearance control design. Established Experimental Construction procedures were employed to perform the work and to ensure that proper responsibilities and methods for the control of various quality standards were followed.

3. EXPERIMENTAL TEST

In Experimental Test, performance calibrations were run on both engines as well as endurance testing on one of the engines. The testing was performed under Experimental Test Department procedures which cover sea level testing in X-8 stand and altitude testing in X-217 stand. Rig tests were run to obtain design substantiation data in the

Middletown and Structures Laboratory Experimental Test facilities. This testing was also performed under Experimental Test Department procedures which cover testing in X-917 stand and the Structures Test Laboratory.

Instrumentation for performance data is provided by Instrumentation Development. Equipment is monitored and controlled by Experimental Test Procedures.

4. INSTRUMENTATION AND EQUIPMENT

Instrumentation and equipment were controlled under the P&WA Quality Assurance Plan which includes controls on the measuring and test equipment in Experimental Test to specific procedures. All testing and measuring equipment carries a label indicating its status (controlled, monitor or calibrated) and, when applicable, the date of calibration and next due date.

The accuracy of gages and equipment used for quality inspection functions was maintained by means of a control and calibration system. The system provided for the maintenance of reference standards, procedures, records, and environmental control when necessary. Gages and tools used for measurements were calibrated utilizing the aforementioned system.

Reference standards were maintained by periodic reviews for accuracy, stability, and range. Certificates of Traceability establish the relationship of the reference standard to standards in the National Bureau of Standards (NBS). Calibration of work standards against reference standards was accomplished in environmental-controlled areas.

Initial calibration intervals for gaging and measuring equipment were established on the basis of expected usage and operating conditions. The computerized gage control system provided a weekly listing of all gages and equipment requiring calibration, highlighting overdue items.

5. DATA

The performance data for the engines in the Experimental test stands was recorded on the Steady State Data System (SSDS), certified to procedures which specified the calibration intervals for the various components requiring laboratory certification. During each data acquisition, the system recorded certified reference parameters which provided an "on-line" verification that the systems were performing properly.

This "confidence" data was reviewed at the time of the run and was later analyzed to provide an overall assessment of the system operations.

The performance data for the rigs in the experimental test stands was recorded manually from instrumentation maintained in accordance with the P&WA quality assurance policy.

6. RECORDS

Quality Assurance personnel ensured that records pertaining to quality requirements were adequate and maintained as directed in Experimental Quality Assurance procedures and in accordance with contractual requirements.

Engine and rig build and operating record books were maintained in accordance with Engineering Department requirements. In addition, a consolidated record of operating times for each rig or component test article used in the experimental program was maintained.

7. RELIABILITY, MAINTAINABILITY AND SAFETY

Standard production engine design techniques and criteria, which consider product reliability and maintainability in context with all other requirements (such as performance, weight and cost), were used in defining the parts for the Improved HPT Active Clearance Control Program. Critical stress and temperature areas of the modified parts were analyzed to ensure that their structural margins were equal to or better than those of the Bill-of-Materials parts. Parts designed in this manner would be expected to pass the 1000 cycle deterioration test of this program. This test was accomplished without difficulty. Consequently, the parts have far greater reliability potential than is necessary for the short term simultated altitude performance test and the slippage rig-test. No reliability problems were experienced in these tests. The maintainability aspects of the modified parts were not verified in this program because the external configuration (plumbing, instrumentation, nacelle wrap, etc.) of the experimental engines used were different from the normal production installation. The reliability and maintainability aspects of the modifications would be verified in an engine development and certification program before release to production.

The parts for the blowing rig were designed exclusively for the test because the rig scale is two times normal size, making standard production engine design techniques inappropriate for this case. However, the nature of the rig allowed the use of conservative stress margins for the test conditions, so reliability was not a problem, as expected.

The safety activities at Pratt & Whitney Aircraft are designed to fully comply with the applicable sections of the Federal Aviation Regulations, Part 33 Air Worthiness Standards: Aircraft Engines, as established by the Federal Aviation Administration.

APPENDIX B

EXPLANATION OF SYMBOLS AND ABBREVIATIONS

A	Incremental flange area
ACC	Active Clearance Control
amp	Amperes
avg	Average
^{o}C	Degrees Centigrade
cm	Centimeters
Conf., Config.	Configuration
Const.	Constant
ECI-PI	Engine Component Improvement - Performance Improvement
^{o}F	Degrees Farenheit
ft	Feet
gal	Gallons
h	Heat transfer coefficient
HPC	High pressure compressor
HPT	High pressure turbine
Hr	Hours
i	Flange increment number
I.D.	Inside diameter
in	Inches
Kg	Kilograms
lbf	Pounds force
lbm	Pounds mass
LPC	Low pressure compressor
LPT	Low pressure turbine
m	Meters
mm	Millimeters
max. cont.	Maximum continuous
MCR	Maximum cruise thrust
min	Minutes
MN	Mach number
Mod	Modification
N	Newtons
N_2	High pressure rotor speed
n	Number of area increments
O.D.	Outside diameter
P&WA	Pratt & Whitney Aircraft
Pa	Pascals
PR	Pressure ratio
psi	Pounds per square inch
Q	Power input
s	Seconds
SSDS	Steady-State Data System
T	Flange temperature
T/C	Thermocouple
T_{air}	Cooling air temperature
Temp.	Temperature
TSFC	Thrust specific fuel consumption
yr	year
z	Impingement distance

REFERENCES

1. Gaffin, W. O. and Webb, D. E., "JT8D and JT9D Jet Engine Component Improvement Program - Task I Feasibility Analysis - Final Report", NASA CR-159449, April 1979

DISTRIBUTION LIST

AFPRO (OL-AA, Det.8)
Pratt & Whitney Aircraft Group
East Hartford, CT 06108
Attn: J. P. Murphy
Chief Quality Performance
Branch

AVCO Lycoming Division
550 South Main Street
Stratford, CT 06497
Attn: A. Bright, Engine. Perform

Aerojet Manufacturing Company
601 S. Placentia
Fullerton, CA 92634
Attn: John Kortenhoeven, VP Eng.

Air Research Manuf. Co.
of Arizona, Dept. 93-010/503-4B
P.O. Box 5217, Phoenix, AZ 85010
Attn: Dr. M. C. Steele

Air Research Manufacturing
Company of Arizona
Dept. 93-200/503-3S
402 South 36th Street
Phoenix, AZ 85010
Attn: Karl R. Fledderjohn
Chief of Fan and Jet
Engines

Air Transport Association
1709 New York Ave., NW
Washington, DC 20056
Attn: E.L. Thomas, Asst.VP. Eng.

Allegheny Airlines, Inc.
Greater Pittsburgh International
Pittsburgh, PA 15231
Attn: William G. Peppler
Director of Engineering

American Airlines, Inc.
Tulsa Maint. & Engrg. Center
N. Mingo Road
Attn: Keith Grayson

American Airlines, Inc.
Tulsa Maintenance & Engineering
Center,
N. Mingo Road
Tulsa, Oklahoma 74151
Attn: Keith Grayson

Arnold Eng. & Devel. Center
AEDC/XRFX
Arnold AFS, TN 39389
Attn: Dr. James G. Mitchell
Dir. of Facility Plans and Prgms

Arnold Eng. & Develop. Center
AEDC/XRFX
Arnold AFS, TN 39389
Attn: R. Roepke

Braniff International
Braniff Tower
P.O. Box 35001
Exchange Park, Dallas, TX 75235
Attn: Hank Nelson
Director, Powerplant
Engineering

Civil Aeronautics Board
Washington, DC 20428
Attn: J. E. Constantz
Chief, Economic Analysis
Division, B-68

Continental Airlines, Inc.
Los Angeles Int. Airport
Los Angeles, CA 90009
Attn: Frank Forster
Director, Powerplant Engrg

Cooper Airmotive, Inc.
4312 Putman Street
Dallas, TX 75235
Attn: Terry Harrison

Delta Airlines, Inc.
Hartsfield-Atlanta Int'l Airport
Atlanta, GA 30320
Attn: Jim Goodrum

Dept. of Transportation
21000 Second St., SW
Washington, DC 20591
Attn: R. S. Zuckerman ARD 550
Aircraft Noise Project Manager

Dept. of Transportation
21000 Second St., SW
Washington, DC 20591
Attn: Harold Ture

Detroit Diesel Allison Div.
General Motors Corp.
P.O. Box 894
Indianapolis, IN 46206
Attn: R. A. Sulkoske
Dept. 8896 MS: V19

Eastern Air Lines, Inc.
Miami Int. Airport
Miami, FL 33148
Attn: P. M. Johnstone
V.P., Engineering

Eastern Air Lines, Inc.
Miami Int. Aiport
Miami, FL 33148
Attn: Max Dow, Director, Pwrplnt
Engineering-MIAEW, Bldg 21

Eastern Air Lines, Inc.
Miami Int. Airport
Miami, FL 33145
Attn: Arthur Fishbein, Sr. Engr
Power Plant Engrg.-MIAEW
Bldg. 21

Federal Aviation Admin.
DOT/FAA/NAFEC
ANA-410, Bldg. 211
Atlantic City, NJ 08405
Attn: Gary Frings
Project Engineer

General Electric Company
Aircraft Engine Group
One Neumann Way
Evandale, OH 45215
Attn: Mr. A. F. Shexnayder
(10 copies)

Hamilton Standard Div. UTC
Windsor Locks, CT. 06096
Attn: Louis A. Urban - Sr. Design
Proj. Eng. MS 3-2-36

Lockheed-California Co.
P.O. Box 551
Burbank, CA 91520
Attn: T. F. Laughlin, Jr.
Director, Aircraft Oper. -
Technology

McDonnell Douglas
3855 Lakewood Blvd.
Long Beach, CA 90846
Attn: Ronald Kawai MC 36-41
Powerplant Engineering

McDonnell Douglas
3855 Lakewood Blvd.
Long Beach, CA 90846
Attn: F. L. Junkermann MC 36-41

McDonnell Douglas
3855 Lakewood Blvd.
Long Beach, CA 90846
Attn: Tech. Library ADTL 246-75

NASA
Washington, DC 20546
Attn: Raymond S. Colladay/RJP-2
(3 copies)

NASA
Washington, DC 20546
Attn: George Deutsch/RT-6

NASA
Washington, DC 20546
Attn: C. R. Nysmith/RP-4

NASA
Langley Research Center
Hampton, VA 23665
Attn: W. J. Alford

NASA
Ames Research Center
Moffett Field, 94035
Attn: L. J. Williams

NASA
Washington, DC 20546
Attn: Dr. John Klineberg/RJB-9

NASA
Washington, DC 20546
Attn: W. S. Aiken/RJ-2

NASA
Washington, DC 20546
Attn: Dr. James Kramer/R-1

NASA
Washington, DC 20546
Attn: R. L. Winblade/RJT-2

NASA
Washington, DC 20546
Attn: Stafford W. Wilbur/RJP-2

NASA
Washington, DC 20546
Attn: R. A. Rudey/RTP-6

NASA
Langley Research Center
Hampton, VA 23665
Attn: Dr. Robert Leonard

NASA
Hugh L. Dryden Flight Rsch. Ctr.
P.O. Box 273, Edwards CA 93523
Attn: Dr. James Albers

NASA Scientific and Technical
Information Facility
Attn: Accessioning Dept.
P.O. Box 8757
Balt/Wash. International Airport
MD 21240 (30 copies)

National Aeronautics & Space Adm
Lewis Research Center
21000 Brookpark Road
Cleveland, OH44135
Attn:Warner L. Stewart/MS 3-5
Director of Aeronautics

National Aeronautics & Space Adm
Lewis Research Center
21000 Brookpark Road
Cleveland, OH 44135
Attn:Joseph A. Ziemianski/
MS 301-4
Manager, Engine Component
Improvement (3 Copies)

National Aeronautics & Space Adm
Lewis Research Center
21000 Brookpark Road
Cleveland, OH 44135
Attn: William J. Anderson/
MS 23-2
Chief, Mechanical
Components Branch

National Aeronautics & Space Adm
Lewis Research Center
21000 Brookpark Road
Cleveland, OH 44135
Attn: Robert W. Hall/MS 49-1
Chief, Materials &
Structures Div.

National Aeronautics & Space Adm
Lewis Research Center
21000 Brookpark Road
Cleveland, OH 44135
Lewis Library/MS 60-3
(2 Copies)

National Aeronautics & Space Adm
Lewis Research Center
21000 Brookpark Road
Cleveland, OH 44135
Attn: Milton A. Beheim/MS 86-1
Chief, Wind Tunnel
& Flight Div.

National Aeronautics & Space Adm
Lewis Research Center
21000 Brookpark Road
Cleveland, OH 44135
Attn: Robert W. Schroeder/
MS 500-207
Chief, V/STOL & Noise Div.

National Aeronautics & Space Adm
Lewis Research Center
21000 Brookpark Road
Cleveland, OH 44135
Attn: Melvin J. Hartmann/MS 5-9
Chief, Fan &
Compressor Branch

National Aeronautics & Space Adm
Lewis Research Center
21000 Brookpark Road
Cleveland, OH 44135
Attn: Salvatore J. Grisaffe/
MS 49-3
Chief, Surface Protection

National Aeronautics & Space Adm
Lewis Research Center
21000 Brookpark Road
Cleveland, OH 44135
Attn: Richard A. Rudey/MS 60-4
Chief, Airbreathing
Engines Div.

National Aeronautics & Space Adm
Lewis Research Center
21000 Brookpark Road
Cleveland, OH 44135
Attn: John E. McAulay/MS 301-4
(13 Copies)

National Aeronautics & Space Adm
Lewis Research Center
21000 Brookpark Road
Cleveland, OH 44135
Attn: Lawrence Ludwig/MS 23-2

National Aeronautics & Space Adm
Lewis Research Center
21000 Brookpark Road
Cleveland, OH 44135
Attn: Tito T. Serafini/MS 49-1

National Aeronautics & Space Adm
Lewis Research Center
21000 Brookpark Road
Cleveland, OH 44135
Report Control Office/MS 5-5

National Aeronautics & Space Adm
Lewis Research Center
21000 Brookpark Road
Cleveland, OH 44135
Attn: Donald L. Nored/MS 301-2
Chief, Energy Conserv.
Engines Office

National Aeronautics & Space Adm
Lewis Research Center
21000 Brookpark Road
Cleveland, OH 44135
Attn: Harold E. Rohlik/MS 77-2
Chief, Turbine Branch

National Aeronautics & Space Adm
Lewis Research Center
21000 Brookpark Road
Cleveland, OH 44135
Attn: Kenneth E. Skeels/
MS 500-305
Contracting Officer

National Airlines, Inc.
P.O. Box 592055
Airport Mail Facility
Miami, FL 33159
R. A. Starner, Director-Engrg.

Naval Air Propulsion Center
1440 Parkway Avenue
Trenton, NJ 08628
Attn: W. L. Pasela (PE-63)
Project Engineer-Test & Eval.

Northwest Airlines, Inc.
Minneapolis-St. Paul Int'l.
Airport
St. Paul, MN 55111
Attn: A. Radosta - MS 838, Ass't
Director, Powerplant
Maintenance

Pacific Airmotive Corp.
2940 N. Hollywood Way
Burbank, CA 91503
Attn: Oddvar Bendikson
Director, Proj. Engrg.

Pacific Airmotive Corp.
2940 N. Hollywood Way
Burbank, CA 91503
Attn: J. R. Gast
Sr. Director Engrg.

Pan American World Airways, Inc.
John F. Kennedy Int. Airport
Jamaica, NY 10430
Attn: Niels Andersen,
Project Engineer

Pan American World Airways, Inc.
John F. Kennedy Int. Airport
Jamaica, NY 10430
Attn: John G. Borger
V.P. & Chief Engineer

Pan American World Airways, Inc.
John F. Kennedy Int. Airport
Jamaica, NY 10430
Attn: Angus MacLarty
Director Pwrplnt. Eng.

Pan American World World Airways
John F. Kennedy Int. Airport
Jamaica, NY 10430
Attn: Robert E. Clinton, Jr.

Piedmont Airlines
Smith Reynolds Airport
Winston-Salem, NC 27102
Attn: H. M. Cartwright, V.P.
Maint. & Engineering

Piedmont Airlines
Smith Reynolds Airport
Winston-Salem, NC 27102
Attn: Paul M. Rehder, Supvsr.
Power Plant Engineering

Seaboard World Airlines, Inc.
Seaboard World Bldg.
JFK Int'l Airport
Jamaica, NY 11430
Attn: Ralph J. Barba
MGR, Pwrplnt. Engrg.

Seaboard World Airlines, Inc.
Seaboard World Bldg.
JFK Int'l Airport
Jamaica, NY 11430
Attn: Jere T. Farrah
VP Maint. and Engrg.

The Boeing Company
P.O. Box 3707
Seattle, WA 98124
Attn: R. Martin MS: 73-07
(2 copies)

The Flying Tiger Line, Inc.
7401 World Way West
Los Angeles Int. Airport
Los Angeles, CA 90009
Attn: B. Lewandowski

The Flying Tiger Line, Inc.
7401 World Way West
Los Angels Int. Airport
Los Angeles, CA 90009
Attn: J. M. Dimin
Manager, Pwrpnt. Engrg.

Trans World Airlines
Kansas City Int. Airport
P.O. Box 20126
Kansas City, MO 64195
Attn: W. D. Sherwood

Trans World Airlines
Kansas City Int. Airport
P.O. Box 20126
Kansas City, MO 64195
Attn: Ken Izumikawa
2-280 MCI

United Airlines, Inc.
San Francisco Int. Airport
San Francisco, CA 94128
Attn: John Curry

United Airlines, Inc.
San Francisco Int. Airport
San Francisco, CA 94128
Attn: James Uhl

Western Air Lines, Inc.
6060 Avion Dr. Box 92,005
World Way Postal Center
Los Angeles, CA 90009
Attn: Walter Holtz

Wright Patterson AFB
Dayton, OH 45433
Attn: E. Bailey, AFAPL/TBD

Wright-Patterson AFB
Dayton, OH 45433
Attn: Major C. L. Klinger,
ASD/YZET

Wright-Patterson AFB
Dayton, OH 45433
Attn: C. M. High, ASD/YZE

Wright-Patterson AFB
Dayton, OH 45433
Attn: E. C. Simpson, AFAPL/TB

Wright-Patterson AFB
Dayton, OH 45433
Attn: Lt. Col. D. S. Dickson,
ASD/YZI